Mechanism and Machine Theory 53 (2012) 99–121

Contents lists available at SciVerse ScienceDirect

Mechanism and Machine Theory

journal homepage: www.elsevier.com/locate/mechmt

Compliant contact force models in multibody dynamics: Evolution of the Hertz contact theory

Margarida Machado [a], Pedro Moreira [a], Paulo Flores [a,*], Hamid M. Lankarani [b]

[a] CT2M/Centro de Tecnologias Mecânicas e de Materiais, Departamento de Engenharia Mecânica, Universidade do Minho, Campus Azurém, 4800-058 Guimarães, Portugal
[b] Department of Mechanical Engineering, Wichita State University, Wichita, KS 67260-133, USA

ARTICLE INFO

Article history:
Received 8 September 2011
Received in revised form 16 February 2012
Accepted 28 February 2012
Available online 28 March 2012

Keywords:
Contact force
Continuous analysis
Hertzian theory
Damping models
Multibody dynamics

ABSTRACT

Over the last decades, several compliant contact force models have been proposed. However, no complete and systematic comparison has been done on these models, which provides information on their range of application and accuracy for use in different contact scenarios. Thus, the selection of an appropriate model for a given contact problem is still an important and challenging issue to be addressed. The Hertzian contact theory remains the foundation for almost all of the available force models, but by itself, it is not appropriate for most impacts in practice, due to the amount of energy dissipated during the impact. A good number of contact force models have been offered that augment the Hertzian law with a damping term to accommodate the energy loss during the impact process for small or moderate impact velocities. In this work, the main issues associated with the most common compliant contact force models of this type are analyzed. Results in terms of the dynamic simulations of multibody systems are presented, which allow for the comparison of the similarities and differences among the models considered.

1. Introduction

One of the problems that faces the designers and engineers in multibody system contact dynamics is how to select the appropriate constitutive law that best describes a given contact–impact event, in the measure that the geometry, the kinematics of the contacting bodies and the nature of the materials involved play a crucial role in the modeling process of contact phenomena [1–3]. A second critical difficulty is associated with the evaluation of the contact parameters, namely the contact stiffness and damping coefficient. These parameters can be evaluated analytically or experimentally [4–6]. Finally, a third problem, that is of complex nature, deals with the quantification of the mechanisms of energy transfer, in particular the loss of energy typically visible by the hysteresis loop in the force–indentation diagrams [7–9]. Therefore, it can be said that the modeling of the interaction between contacting bodies for multibody dynamic simulations is critical for the systems performance [10–14].

It is known that nonsmooth systems exhibit nonlinearities or discontinuities, such as those caused by impacts in clearance joints [15] and intermittent contacts [16]. In nonsmooth systems, the time evolution of the velocities is not requested to be smooth [17]. For instance, the jumps in the velocities that can be caused by impacts in multibody systems represent a typical nonsmooth system [18]. The term regularized deals with the reformulation of a problem to derive a solvable formulation [19]. The contact forces can be described as a function of the indentation by smoothening the discontinuity of impact forces. For instance, the contact force law based on the Hertzian contact theory is a regularization of the contact force problem [20]. Thus, for conceptual clarity the behavior of colliding bodies can roughly be divided into two main groups, namely the nonsmooth dynamics formulation and the regularized approach [21]. Each of these methodologies has peculiar advantages and disadvantages for various

* Corresponding author. Tel.: +351 253510220; fax: +351 253516007.
E-mail addresses: margarida@dem.uminho.pt (M. Machado), pfsmoreira@dem.uminho.pt (P. Moreira), pflores@dem.uminho.pt (P. Flores), hamid.lankarani@wichita.edu (H.M. Lankarani).

0094-114X/$ – see front matter © 2012 Elsevier Ltd. All rights reserved.
doi:10.1016/j.mechmachtheory.2012.02.010

problem classes. The first group is based on geometrical constraints [22] and it is also known as rigid approach, in the measure that the colliding bodies are hard enough to not deform [23]. In turn, the regularized approach is based on the evaluation of the contact forces as function of indentation and compliance of the contacting surfaces, reason why it is often named as compliant, penalty or force based formulation. In contrast to nonsmooth formulations, the regularized models are considered as deformable approaches because the colliding bodies are allowed to deform at the contact zone [24]. Owing to its nature of continuous evaluation of the contact forces as function of the indentation, the regularized models are also referred to as continuous analysis, in contrast with the discrete nature of the nonsmooth formulation [25].

The linear complementarity problem (LCP) is one of the most popular techniques to treat contact–impact events within the context of nonsmooth dynamics formulation [26]. Assuming that the contacting bodies are truly rigid, as opposed to locally deformable or penetrable bodies as in the regularized approach, the complementarity formulation resolves the contact dynamics problem using the unilateral constraints to compute contact impulses to prevent penetration from occurring. Thus, at the core of the complementarity approach is an explicit formulation of the unilateral constraints between the contacting rigid bodies [27]. The basic idea of complementarity in multibody systems can be stated as for a unilateral contact either relative kinematics is zero and the corresponding constraint impulses are zero, or vice versa. The product of these two groups of quantities is always zero. This leads to a complementarity problem and constitutes a rule that allows the treatment of multibody systems with unilateral constraints [28]. In short, in the LCP approach, unilateral constraints are used to deal with the contact problem, main feature of which is the impenetrability concept, that is, the unilateral constraints are utilized to avoid the overlap of the contacting bodies, meaning that the contact points must not cross the boundaries of antagonist bodies. Additionally, it is also assumed that the bodies are not attracting each other, that is, the impulsive forces are nonnegative, being vanished when the contact is not active. This makes the contact process analysis efficient from the computational point of view. However, with this approach it is required different numerical strategies for different contact scenarios, such as permanent contact and intermittent impact [26]. Furthermore, in the presence of Coulomb friction the contact problem can exhibit multiple solutions or no solution [29]. Another drawback can be associated with the LCP formulation, namely the possible violation of energy conservation principle during contacts with friction [30]. Moreover, the LCP approach is not easy to implement in a general-purpose program for multibody dynamics [31].

The compliant contact force models do not suffer from these difficulties. For instance, the regularized models provide a unique approach for modeling continuous and intermittent contacts, being able to handle impacts, sustain contacts under load conditions and transitions from and to contact conditions [32]. The regularized formulations can be understood as if each contact region of the contacting bodies is covered with some spring-damper elements scattered over their surfaces. The normal force, that includes elastic and damping terms, prevents penetration, i.e., no explicit kinematic constraint is considered but simply force reaction terms are used. The magnitudes of stiffness and deflection of the spring-damper elements are computed based on the relative indentation, material properties and surface geometries of the colliding bodies. One of the main drawbacks associated with the compliant force models is the difficulty to choose the contact parameters such as the equivalent stiffness and the degree of nonlinearity of the indentation, especially for complex contact scenarios and nonmetallic materials. In compliant force models, the contact force is expressed as a continuous function of indentation between the contacting bodies, being quite simple and straightforward to implement in general-purpose multibody codes. Over the last few decades, several different compliant force models have been published in the literature to represent the interaction between contacting bodies [33]. Some of them are purely elastic in nature, while others include dissipative terms that are typically formulated as a function of the coefficient of restitution and impact velocity. The dissipative force models consist of an association of spring and damper elements with linear or nonlinear force characteristics, being the amount of energy dissipation associated with the internal damping of materials. The utility of some models developed to date is somewhat restrict because they are valid for coefficients of restitution close to unity [34]. Gonthier et al. [35] and Flores et al. [36] are among the few who have proposed compliant force models valid for a wide range of coefficient of restitution values. In short, it can be said that the compliant contact force models have been gaining significant importance in the context of multibody systems with contact–impact events due to their computational simplicity and efficiency. In addition, the compliant contact force models contribute to an efficient integration of the equations of motion and account for some level of energy dissipation. This amount of good reasons explains why some of the most popular commercial multibody codes use the penalty methods to treat contact problems [37–39].

It is important to mention that the bodies that belong to a multibody system can be considered as rigid or deformable. A body is said to be rigid when its deformations are assumed to be small such that they do not influence the global motion produced by the body. The expression deformable multibody system refers to a system holding deformable bodies with internal dynamics [40]. In fact, rigid bodies are a representation of reality because bodies are not absolutely rigid in nature. However, many physical mechanical systems contain a combination of rigid and deformable bodies, or rigid bodies with soft surfaces, or bodies that are rigid enough to be considered rigid overall, but soft enough to experience significant local deformations during contact. In this case, the contact approach must be able to model the dynamics of contact between compliant surfaces [41].

When two bodies collide initially the force increases with increasing indentation and it reduces the velocity at which the bodies are approaching each other. At some instances during the impact process the work done by the contact force is sufficient to bring the approaching velocity of the two bodies to zero. This corresponds to the end of the compression or loading phase where the indentation reaches its maximum value. Subsequently, part of the energy stored during the compression drives the two bodies to apart until finally they separate with some relative velocity. Moreover, part of the energy of deformation is dissipated in many forms such as heat, vibration, sound and so forth [42]. In a simple manner, the several different mechanisms by which the contact energy dissipation occurs can be named as internal damping [43]. Even the collisions at very low velocity with perfectly elastic deformation can dissipate energy, since initial rigid body kinetic energy can be converted to internal vibration and waves that persist after contact ends [44]. In general, when modeling contact–impact events within the framework of multibody systems formulations, the energy dissipation is controlled by the coefficient of restitution [45]. This parameter has different definitions, being one of the most popular and commonly used the Newton's law of restitution, also known as kinematical coefficient of restitution. In a simple manner, this definition states that when two bodies collide, the post-impact velocity is related to the pre-impact velocity by a constant of proportionality called coefficient of restitution. This coefficient is, in general, assumed to be constant, however, it is dependent on several factors such as the geometry of the contacting surfaces, pre-impact velocity, local material properties, contact duration, temperature and friction [46–48].

The prediction of the dynamic behavior of multibody mechanical systems involves the formulation of the governing equations of motion and the evaluation of their kinematic and dynamic characteristics. This desideratum is reached when all the necessary ingredients that influence the response of the multibody systems are adequately taken into account. The contact–impact phenomenon is among the most important and complex to model because they are dependent on many factors, such as the geometry of the contacting bodies, the material properties and the constitutive law used to represent the interaction among the different bodies that comprise the multibody systems. The classical problem of the contact mechanics is a rather old topic in engineering applications. The pioneering work on the collision between rigid bodies was developed by Hertz [49]. Naturally, the following step was to include the energy dissipation in terms of damping component on the contact analysis. Despite its long and profitable history, multibody system contact mechanics is still an active challenging research domain, as stated by Schiehlen "more work is required to better understand the micromechanical phenomena influencing the macromechanical multibody motion with contact" [50]. Thus, the main purpose of this work is to present and discuss several different compliant contact forces models used in the context of multibody system dynamics to model and analyze contact–impact events. Special emphasis is paid on the evolution of the Hertz contact theory, being the most common continuous elastic and dissipative contact force models examined and their performances evaluated. The similarities and differences for several contact force models are also investigated. Results obtained from computational simulations are presented and utilized to discuss the main assumptions and limitations associated with the several contact force models analyzed throughout this study.

The remaining of the paper is organized as follows. In section 2, a brief revision of the multibody systems formulation is offered. The fundamental issues associated with the generalized contact kinematics are described in section 3. Then, several pure elastic and dissipative contact force models are presented in sections 3 and 5, respectively. Section six includes some global results of dynamics of multibody systems involving frictionless contact–impact events. Finally, in the last section, the main conclusions from this study are drawn and the perspectives for future research are outlined. The engineering analysis and design implications of the obtained analysis can thus be observed.

2. Description of multibody systems formalism

The dynamic analysis of multibody systems, made of interconnected bodies that undergo large displacements and rotations, is a research area with applications in a broad variety of engineering fields that has been deserved significant attention over the last few decades, which led to the development of relevant work and even to the publication of a good number of textbooks totally devoted to this topic [51–56]. The fundamental approaches of analytical and recursive dynamics for rigid and flexible bodies have been summarized and discussed in several review papers over the last years, such as those by Schiehlen [57,58], Shabana [59], Rahnejat [60], Eberhard and Schiehlen [61], Jalón [62], Nikravesh [63], among others. In turn, many multibody computational programs capable of automatic generation and integration of the differential equations of motion have been developed, namely DAP [52], ADAMS [37], COMPAMM [64], SIMPACK [65] or NEWEUL [66]. The various formulations of multibody systems used in these programs differ in the principle used, (e.g. principle of virtual work, principle of virtual power, Newton–Euler approach), types of coordinates adopted, (e.g. Cartesian coordinates, natural coordinates) and the method selected for handling constraints in systems characterized by closed loop topology (e.g. Baumgarte stabilization technique, coordinate partitioning method, augmented Lagrange formulation) [67–69].

There are different coordinates and formalisms that lead to suitable descriptions of multibody systems, each of them presenting relative advantages and drawbacks. In the present work, the generalized Cartesian coordinates and the Newton–Euler approach are used in the multibody formulation that support the modeling and simulation of mechanical systems with contact–impact events. This formulation results in the establishment of a mixed set of partial differential and algebraic equations, which are solved in order to predict the dynamic behavior of multibody systems. The Newton–Euler approach is very straightforward in terms of assembling the equations of motion and providing all joint reaction forces. Additionally, the equations of motion are solved by using the Baumgarte stabilization technique with the intent of keeping the constraints violation under control [67,70]. This method can be understood as an extension of the feedback control theory applied to the dynamics of multibody systems. Moreover, in the present work, the numerical problems that arise from the existence of redundant constraints and the possibility of achieving singular positions are assumed to be solved [71]. In turn, the integration process is performed by using a numerical algorithm with variable order and time step [72]. The methodologies used in this study have been implemented in the computational program MUBODYNA [73]. This multibody formulation code is capable of automatically generating and solving the equations of motion for general planar multibody systems.

A typical multibody system is defined as a collection of rigid and/or flexible bodies interconnected by kinematic joints and possibly some force elements [52]. Driving elements and prescribed trajectories for given points of the system components can also be represented under this general concept of multibody system. Fig. 1 depicts an abstract representation of a multibody system. The bodies that belong to a multibody system can be considered as rigid or flexible. A body is said to be rigid when its deformations are assumed to be small such that they do not affect the global motion produced by the body. In the two-dimensional space, the motion of a free rigid body can be fully described by three generalized coordinates associated with the three degrees-of-freedom. In turn, when a body

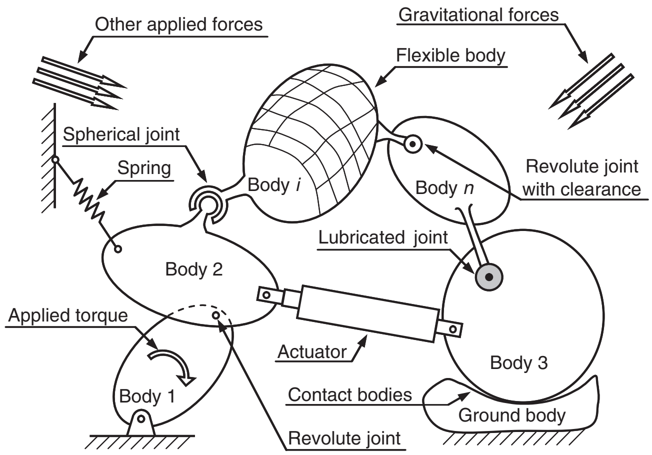

Fig. 1. Abstract representation of a multibody system with its most significant components: bodies, joints and forces elements.

includes some amount of flexibility, it has three rigid degrees-of-freedom plus the number of generalized coordinates necessary to describe the deformations [40]. Within the scope of the present work, only rigid bodies are considered.

Multibody systems can range from very simple to highly complex. In fact, a multibody system can be used to study the kinematic and dynamic motion characteristics of a wide variety of systems in a large number of engineering fields of application. There is no doubt that multibody systems are ubiquitous in engineering and research activities, such as robotics [74], automobile vehicles [75], biomechanics [76], mechanisms [77], railway vehicles [78], space systems [79], just to mention a few. In a simple way, multibody systems methodologies include the following two phases: (*i*) the development of mathematical models of systems and (*ii*) the implementation of computational procedures to perform the simulation, analysis and optimization of the global motion produced [56].

For a constrained multibody system, the kinematic joints can be described by a set of typically nonlinear holonomic algebraic equations as [52]

$$\boldsymbol{\Phi}(\mathbf{q}, t) = \mathbf{0} \tag{1}$$

where $\mathbf{q}$ is the vector of generalized coordinates and t is the time variable. Differentiating Eq. (1) with respect to time yields the velocity constraint equations. After a second differentiation with respect to time, the acceleration constraint equations are obtained as

$$\boldsymbol{\Phi}_{\mathbf{q}}\ddot{\mathbf{q}} = \boldsymbol{\gamma} \tag{2}$$

in which $\boldsymbol{\Phi}_{\mathbf{q}}$ is the Jacobian matrix, $\ddot{\mathbf{q}}$ is the acceleration vector and $\boldsymbol{\gamma}$ is the right-hand side of acceleration equations, which contains the terms that are exclusively functions of velocity, position and time.

The translational and rotational equations of motion for an unconstrained multibody system composed by rigid bodies are written as [52]

$$\mathbf{M}\ddot{\mathbf{q}} = \mathbf{g} \tag{3}$$

where $\mathbf{M}$ is the global system mass matrix, containing the mass and moments of inertia of all bodies and $\mathbf{g}$ is the generalized force vector that contains all external forces and moments applied on the system, such as those associated with gravitational field and contact–impact events [80]. Using the Lagrange multipliers technique, the effect of the constraint equations (1) is added to the equations of motion (3) [81]. Thus, the equations of motion are written together with the second time derivative of constraint equations (2) yielding a linear system of equations written as

$$\begin{bmatrix} \mathbf{M} & \boldsymbol{\Phi}_{\mathbf{q}}^T \\ \boldsymbol{\Phi}_{\mathbf{q}} & \mathbf{0} \end{bmatrix} \begin{Bmatrix} \ddot{\mathbf{q}} \\ \boldsymbol{\lambda} \end{Bmatrix} = \begin{Bmatrix} \mathbf{g} \\ \boldsymbol{\gamma} \end{Bmatrix} \tag{4}$$

where $\boldsymbol{\lambda}$ is the vector of Lagrange multipliers, physically related to the joint reaction forces. The reaction forces, owing to the kinematic joints are expressed as [82]

$$\mathbf{g}^{(c)} = -\boldsymbol{\Phi}_{\mathbf{q}}^T\boldsymbol{\lambda} \tag{5}$$

Eq. (4) represents a differential-algebraic system that has to be solved and the resulting accelerations integrated in time. This method, however, does not explicitly use the position and velocity constraint equations allowing for a drift in the system constraints to develop. In order to keep such constraint violation during the numerical integration under control, the Baumgarte stabilization technique is employed, and Eq. (4) is modified as

$$\begin{bmatrix} \mathbf{M} & \mathbf{\Phi}_{\mathbf{q}}^T \\ \mathbf{\Phi}_{\mathbf{q}} & \mathbf{0} \end{bmatrix} \begin{Bmatrix} \ddot{\mathbf{q}} \\ \boldsymbol{\lambda} \end{Bmatrix} = \begin{Bmatrix} \mathbf{g} \\ \boldsymbol{\gamma} - 2\alpha\dot{\mathbf{\Phi}} - \beta^2\mathbf{\Phi} \end{Bmatrix} \tag{6}$$

where α and β are prescribed positive constants that represent the feedback control parameters for the velocities and positions constraint violations [67,70].

According to this formulation, the dynamic response of multibody systems involves the evaluation of the vectors $\mathbf{g}$ and $\boldsymbol{\gamma}$, for each time step. Then, Eq. (6) is solved for the system accelerations $\ddot{\mathbf{q}}$. These accelerations together with the velocities $\dot{q}$ are integrated in order to obtain the new velocities $\dot{q}$ and positions $\mathbf{q}$ for the next time step. This process is repeated until the complete description of system motion is performed [52,83,84].

3. Generalized contact kinematics

This paragraph deals with the generalized contact kinematics between two planar rigid bodies that can experience an oblique eccentric impact. Fig. 2a shows two convex bodies i and j in the state of separation that are moving with absolute velocities $\dot{\mathbf{r}}_i$ and $\dot{\mathbf{r}}_j$, respectively. The potential contact points are denoted by P_i and P_j. The evaluation of the contact kinematics involves the calculation of three fundamental quantities, namely the position of the potential contact points, their Euclidian distance and their relative normal velocity [85,86]. In general, this information must be available in order to allow the determination of the contact forces that develop during the contact–impact events [87,88]. The possible motion of each body in a multibody system is constrained by the distance and relative velocity of the potential contact points. Positive values of that distance represent a separation, while negative values denote relative indentation or penetration of the contacting bodies. These two scenarios are illustrated in Fig. 2a and b, respectively. The change in sign of the normal distance indicates a transition from separation to contact, or vice-versa [89]. In turn, positive values of the relative normal velocity between the contact points, that is, the indentation or penetration velocity, indicate that the bodies are approaching, which corresponds to the compression phase, while negative values denote that the bodies are separating, that corresponds to the restitution phase. The vectors of interest in studying contact–impact events are shown in Fig. 2.

The vector that connects the two potential contact points, P_i and P_j, is a gap function that can be expressed as

$$\mathbf{d} = \mathbf{r}_j^P - \mathbf{r}_i^P \tag{7}$$

where both $\mathbf{r}_i^P$ and $\mathbf{r}_j^P$ are described in global coordinates with respect to the inertial reference frame [52], that is,

$$\mathbf{r}_k^P = \mathbf{r}_k + \mathbf{A}_i \mathbf{s}_i' P \quad (k = i, j) \tag{8}$$

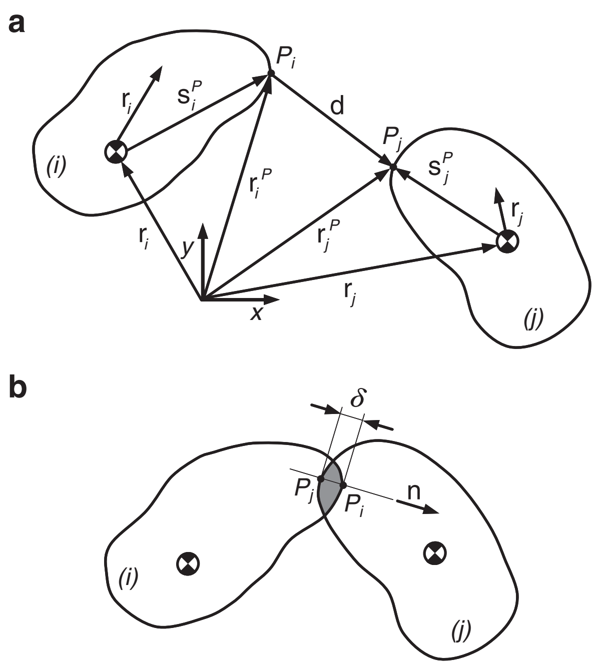

Fig. 2. (a) Two bodies in the state of separation; (b) two bodies in the state of contact (indentation).

in which $\mathbf{r}_i$ and $\mathbf{r}_j$ represent the global position vectors of bodies i and j, while $\mathbf{s}_i^{'P}$ and $\mathbf{s}_j^{'P}$ are the local components of the contact points with respect to local coordinate systems. The rotational transformation matrices $\mathbf{A}_k$ are given by

$$\mathbf{A}_k = \begin{bmatrix} \cos\phi_k & -\sin\phi_k \\ \sin\phi_k & \cos\phi_k \end{bmatrix} \quad (k = i, j) \tag{9}$$

A normal vector to the plane of contact, illustrated in Fig. 2b, can be determined as

$$\mathbf{n} = \frac{\mathbf{d}}{d} \tag{10}$$

where the magnitude of the vector $\mathbf{d}$ is evaluated as

$$d = \mathbf{n}^T \mathbf{d} \tag{11}$$

The minimum distance condition given by Eq. (11) is not enough to find the possible contact points between the contact bodies, since it does not cover all possible scenarios that may occur in the contact problem. Therefore, the contact points are defined as those that correspond to maximum indentation, that is, the points of maximum relative deformation, measured along the normal direction [90]. Thus, three geometric conditions for contact can be defined as, (i) the distance between the potential contact points given by vector $\mathbf{d}$ corresponds to the minimum distance; (ii) the vector $\mathbf{d}$ has to be collinear with the normal vector $\mathbf{n}_i$; (iii) the normal vectors $\mathbf{n}_\mathrm{i}$ and $\mathbf{n}_\mathrm{j}$ at the potential contact points have to be collinear. The conditions (ii) and (iii) can be written as two cross products as

$$\mathbf{n}_j \times \mathbf{n}_i = \mathbf{0} \tag{12}$$

$$\mathbf{d} \times \mathbf{n}_i = \mathbf{0} \tag{13}$$

The geometric conditions given by Eqs. (12) and (13) are two nonlinear equations with two unknowns, which can be solved using a Newton–Raphson iterative procedure [84]. This system of equations provides the solutions for the location of the potential contact points. Once the potential contact points are found, the next step deals with the evaluation of the relative indentation between the contact bodies as

$$\delta = \sqrt{\mathbf{d}^T \mathbf{d}} \tag{14}$$

The velocities of the contact points expressed in terms of the global coordinate system are evaluated by differentiating Eq. (8) with respect to time, yielding

$$\dot{\mathbf{r}}_k P = \dot{\mathbf{r}}_k + \dot{\mathbf{A}}_k \mathbf{s}_k^{'P} \quad (k = i, j) \tag{15}$$

in which the dot denotes the derivative with respect to time.

The relative normal velocity is determined by projecting the contact velocity onto the direction normal to the plane of contact, yielding

$$v_N = \dot{\delta} = \mathbf{n}^T \left(\dot{\mathbf{r}}_j^P - \dot{\mathbf{r}}_i^P \right) \tag{16}$$

This way to represent the relative normal velocity is very convenient, in the measure that it is not necessary to deal with the derivation of the normal unit vector because this velocity component is not directly obtained by differentiating Eq. (11). Furthermore, the fully rigid body velocity kinematics can easily be applied.

The computational implementation of this methodology is quite efficient. However, the above description is restricted to convex rigid bodies with a smooth surface at least in a neighborhood of the potential contact points such that the contact area reduces to a single point which may move relative to the surfaces of the bodies. This approach can be extended to more generalized contact geometries as long as a common tangent plane of the contacting bodies is uniquely defined [91].

4. Pure elastic contact force models

This section briefly covers the analytical formulation of, and the limitations with, the pure elastic contact force models based on the Hertzian contact theory. Hertz was pioneer to study the contact stresses between two perfectly elastic bodies, when he was investigating on the Newton's optical interface fringes in the gap between two glass lenses and was concerned with the possible influence of the deformation of the surfaces of the lenses due to the contact pressure between them [49]. Hertz concluded that the contact area was, in general, elliptical. For a detail description of the Hertzian contact theory, the reader is referred to the thematic literature [20,43,92]. The Hertz's law relates the contact force with a nonlinear power function of indentation and can be expressed as

$$F_N = K\delta^n \tag{17}$$

where δ represents the relative indentation between the contacting bodies, K and n are the contact stiffness parameter and the nonlinear power exponent determined from material and geometric properties of the local region of the contacting objects. One advantage of the Hertz contact law is that it considers the geometric and material characteristics of the contacting surfaces, which are of paramount importance in the contact dynamic responses. For instance, for two spheres of isotropic materials in contact, the contact stiffness parameter is a function of the radii of the sphere i and j and the material properties as [43]

$$K = \frac{4}{3\left(\sigma_i + \sigma_j\right)} \sqrt{\frac{R_i R_j}{R_i + R_j}} \tag{18}$$

in which the material parameters σ_i and σ_j are given by

$$\sigma_l = \frac{1 - \nu_l^2}{E_l}, \ \ (l = i, j) \tag{19}$$

and the quantities ν_l and E_l are the Poisson's ratio and Young's modulus associated with each sphere. For contact between a sphere i and a plane surface body j, the contact stiffness parameter depends on the radius of the sphere and the material properties of the contacting surfaces, being expressed as

$$K = \frac{4}{3\left(\sigma_i + \sigma_j\right)} \sqrt{R_i} \tag{20}$$

It is must be noted that, by definition, the radius is negative for concave surfaces and positive for convex surfaces [93]. According to Hertzian contact approach, the power exponent n is equal to 3/2 for the case where there is a parabolic distribution of contact stresses [49]. For different materials, the value of this exponent can be either higher or lower, leading to a convenient contact force expression which is based on experimental work, but that should not be confused with the Hertzian contact theory [94,95]. Guess and Maletsky [96] utilized the Hertzian contact approach to evaluate the contact forces that develop in the tibiofemoral and patellofemoral connections within a dynamic knee multibody simulator for modeling total knee prosthesis. In this work, Guess and Maletsky used the value of 3/2 for the nonlinear exponent, while the contact stiffness parameter was evaluated based on the material properties and surface geometries of the contact elements.

For the Hertz contact law, Fig. 3 shows the contact force, the indentation, the force–indentation relation and the phase portrait of two externally colliding spheres. The contact indentation and the indentation velocity are the variables used to plot the phase portrait. The spheres are identical and have the same radius of 20 mm and the same mass of 0.092 kg. Both spheres have equal and opposite impact velocities of 0.15 m/s. The relative contact stiffness parameter is equal to 5.5×10^9 N/m$^{3/2}$ for the calculations used to generate the plots [97]. By observing the plots of Fig. 3, it should be highlighted that the contact force varies in a nonlinear and continuous manner and it starts from zero and returns to zero while always remaining compressive. Fig. 3c depicts the phase trajectory of the impact process, in which point A denotes the initial instance of impact with null indentation and impact velocity equal to 0.3 m/s. The segment AB corresponds to the compression phase that ends at point B, where the maximum relative indentation is reached. Finally, the segment BC represents the restitution phase, which terminates with relative velocity equal to -0.3 m/s and null indentation. It is apparent that the Hertz contact law given by Eq. (17) is limited to contacts with pure elastic deformations and does not include energy dissipation. This contact force model represents the contact process as a nonlinear spring along the direction of collision.

One limitation associated with the Hertz's law deals with the evaluation of the contact stiffness parameter and nonlinear exponent, particularly when the bodies contact in a line or surface instead of a point [93,98,99]. In fact, for spherical contact geometries, where the contact areas assume a circular or ellipsoidal shape, the contact stiffness parameter used to define the constitutive contact force law is estimated by applying the Hertz theory of contact. However, for rectangular contact areas, that is, for contacts involving cylindrical shape bodies with parallel axis, the physical meaning of the contact stiffness parameter is not straightforward and its value is not easy to obtain. In empirical and theoretical investigations, Brändlein and his co-authors [100] proposed the following mathematical relation for the contact between cylinders

$$F_N = K\delta^{1.08} \tag{21}$$

It is worth to note that K depends on the contact length and is independent of the contact radii of the bodies. A similar force–indentation relation for the contact between a cylinder of infinite length and a half space was presented by Nijen [101].

After an extensive review of the Hertz contact theory, Goldsmith [43] concluded that the Hertz theory provides a good model of the contact process if the materials involved are hard and the initial impact velocity is very low, that is, impacts slow enough that the bodies are deformed imperceptibly only. For softer materials or higher impact velocities, plastic deformation and strain rate effects must be included [44,94,102]. Goldsmith proposed a modified Hertz's law to accommodate plastic or permanent indentation during the restitution phase as [43]

$$F_{\mathrm{N}} = F_{\max}\left(\frac{\delta - \delta_{\mathrm{p}}}{\delta_{\max} - \delta_{\mathrm{p}}}\right)^n \tag{22}$$

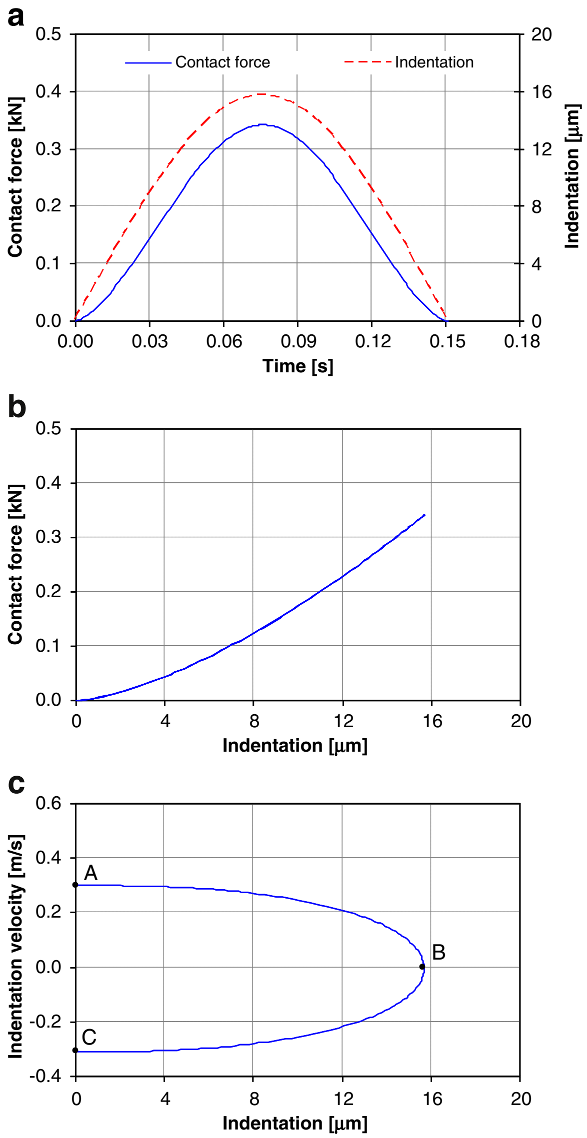

Fig. 3. Externally colliding spheres modeled by Hertz contact law: (a) contact force and indentation versus time; (b) force–indentation relation; (c) phase portrait.

where F_{max} denotes the maximum contact force, δ_{max} is the maximum indentation and δ_p represents the permanent indentation. A straightforward manner to evaluate these parameters can be found in work by Lankarani and Nikravesh [97].

Yang and Sun [103] linearized the Hertz's law to model the contact force developed in spur gear dynamics, yielding the following expression

$$F_N = K\delta \tag{23}$$

in which the contact stiffness is given by

$$K = \frac{\pi EL}{4(1-\nu^2)} \tag{24}$$

where E is the Young's modulus, ν is the Poisson's ratio and L denotes the thickness of the gears. Dubowsky and Freudenstein [104] also considered a linear relation between indentation and contact force for the case of contact of a journal inside of a bearing when the impact takes place at low velocity and the loads involved are small. The linearization of the Hertz's law may not be very accurate because it does not represent the overall nonlinear nature of an impact, and a number of weaknesses limit its application as it was avowed by Hunt and Crossley [7].

Another weakness associated with Hertz's law is that it assumes that the size of contact area is small when compared to the curvature radii of the surfaces in contact. This assumption seems good enough for nonconformal contacts. However, for the case of conformal contacts this is not entirely true due to the large deformations that occur at the contact zone [20]. Goodman and Keer [105] demonstrated that conformal contacts can be up to 25% stiffer in compression than would be predicted by the Hertzian contact theory. This idea has been corroborated by Pereira and her co-authors [99]. Liu et al. [106] extended the Hertz contact law to propose a new force model for the particular case of spherical joints with clearance. In a previous work, Liu and his co-workers [107] presented a compliant force model for cylindrical joints with clearances, where the Hertz's law is only valid for large clearance sizes and small loads [104,108]. The force model proposed by Liu et al. [107] can be expressed as

$$F_{\mathrm{N}} = \frac{\pi E^{*} L \delta}{2}\left(\frac{\delta}{2(c+\delta)}\right)^{\frac{1}{2}} \tag{25}$$

where E^* represents the composite modulus of the two colliding cylinders, L is the length of cylindrical joint, δ denotes the relative indentation and c is the radial clearance size. This approach was compared and validated with results obtained with FEM analysis [109]. The composite modulus can be evaluated using the following mathematical expression

$$E^{*} = \left(\frac{1-\nu_i^2}{E_i} + \frac{1-\nu_j^2}{E_j}\right)^{-1} \tag{26}$$

More recently, Luo and Nahon [110] extended the Hertz contact approach for polyhedral contacting bodies, namely for line and face contacting objects, in which they explicitly consider the distinction between true contact geometry and interference geometry. This new approach was accompanied with both FEM and experimental discussions. Another way to overcome the difficulties of the Hertz's law, when the contact area cannot be represented as a single contact point, is to consider the elastic foundation approach [88]. This model is based on representation of the body surfaces by polygon meshes and contact force determination by the elastic foundation model, which allows for the modeling of contact between complex geometries and scenarios where the contact area is relatively large, having good computational efficiency when compared with the FEM analysis. Bei and Fregly [111] proposed a computationally efficient methodology for combining multibody dynamic simulation method with a deformable contact knee model. In this study, the contact between knee surfaces was modeled through the use of the elastic foundation approach for both natural and artificial knee articulations. Pérez-González et al. [112] developed a modified elastic foundation approach for application in three-dimensional models of the prosthetic knees, in which both contacting bodies are considered to be deformable solids with their own elastic properties. Mukras et al. [113] also used the elastic foundation method to evaluate the contact forces for wear modeling and analysis in the framework of multibody systems formulations. Their results obtained for a planar slider-crank mechanism with a dry clearance revolute joint were compared and validated with those produced via FEM.

At this stage, it must be highlighted that the contact force models described above do not consider the energy dissipation during the contact process. In fact, the process of energy transfer is an extremely complex task of modeling contact–impact events. When an elastic body is subjected to cyclic loads, the energy loss due to internal damping causes a hysteresis loop in the force–indentation diagram, which corresponds to energy dissipation. Krempf and Sabot [114] identified the damping capability of a dry sphere pressed against a plate made by steel (Hertzian contact) from experimental nonlinear resonance curves. These authors observed that the contact damping shows approximately viscous behavior (Kelvin and Voigt like). This corresponds to the theoretical considerations presented by Hunt and Crossley [7]. Sabot et al. [115] experimentally studied a ball normally preloaded by a moving rigid mass. They clearly exhibited the softening primary resonance when no loss of contact occurs and analyzed mechanical sources of damping. In a similar manner to Krempf and Sabot, Johnson [116] measured the energy loss within a dry contact, in which two spherical surfaces were pressed together and excited by an oscillating force. The force direction deviates from the normal direction to the contact plane, and notable energy dissipation was observed. The fundamental issues associated with internal damping that occurs in the contact process will be analyzed and discussed in the next section.

5. Dissipative contact force models

The pure elastic contact force models presented in the previous section do not account for the energy dissipation process that characterizes the contact–impact events in mechanical systems. Therefore, the Hertz contact model cannot be used during the compression and restitution phases of contact. This issue has led several researchers to extend the Hertz's law to accommodate energy dissipation in the form of internal damping. In particular, the models proposed by Hunt and Crossley [7] and Lankarani and Nikravesh [34] are two examples of extensive use to model, simulate and analyze multibody systems involving contacts.

The Kelvin and Voigt approach is one of the first dissipative contact force models that combines a linear spring with a linear damper [43]. These two elements are associated in parallel, and the contact force model can be written as

$$F_{\mathrm{N}} = K\delta + D\dot{\delta} \tag{27}$$

in which the first term of the right-hand side is referred to as the linear elastic force component (Hooke type behavior [117]) and the second term accounts for the energy dissipation during the contact process. In Eq. (27), the parameter D denotes the damping coefficient of the damper element and $\dot{\delta}$ represents the relative normal contact velocity, and the remaining variables have the same meaning as it was described in the previous section.

Besides its simplicity and some weaknesses, the Kelvin and Voigt model has been used by a good number of researchers. Dubowsky and his co-workers [104,118–120] employed this approach to evaluate the interbody contact forces that develop in elastic mechanisms with spatial clearance joints. These authors also stated that the selection of the compliance and damping coefficients are dependent on the materials and dimensions of the elements involved in the contact. Additionally, Dubowsky and Young [121] provided some experimental data that supports the successful use of the Kelvin and Voigt model in the case of a revolute joint subjected to one-dimensional vibroimpact. Rogers and Andrews [122] also applied this contact force model to dynamically simulate planar mechanical systems with impacts at revolute clearance joints. They argued that this contact force model can be a satisfactory approximation of a viscoelastic nature when the material damping is very slight. However, for higher degrees of material damping, a better formulation would have the damping force proportional to the product of velocity and the elastic force. Khulief and Shabana [123] utilized a parallel linear spring-damper element combination of Kelvin and Voigt type to model impact in mechanisms with flexible multibody systems. Hegazy et al. [124] used the Kelvin and Voigt contact force model to compute the vertical forces developed at the tire in the context of multibody dynamics of a full vehicle handling analysis. A similar application was done by Fox et al. [125]. However, these authors highlighted that the improvement of the contact force model is a fundamental concern to predict accurate dynamic responses of this type of multibody systems.

In short, the linear Kelvin and Voigt force model may not be very accurate since it does not represent the overall nonlinear nature of an impact, and a number of weaknesses limit its application, mainly for high impact velocities. Dubowsky et al. [126] suggested that the compliance and damping force components must be expressed as nonlinear functions of the relative indentation and impact velocity. Furthermore, the Kelvin and Voigt contact force model has other weaknesses, namely the fact that the contact force at the beginning of the contact is not continuous due to the existence of the damping component. This particular issue is not realistic because when the contact begins, both elastic and damping force components must be null. Moreover, at the end of the restitution phase, the penetration is null, the relative contact velocity is negative and, consequently, the resulting contact force is also negative. This situation does not make sense from the physical point of view, in the measure that the bodies cannot attract each other. Another limitation of the Kelvin and Voigt model is that its damping force component is active with the same damping coefficient during the entire impact time interval. This results in uniform dissipation during the compression and restitution phases, which is not fully consistent with reality [24,87,127].

Thus, a more physical and realistic model is demanded. For instance, Hunt and Crossley [7] have argued that the damping coefficient in the case of vibroimpact should be proportional to a power of the spring force. These authors also showed that the linear Kelvin and Voigt approach does not represent the physical nature of the energy transferred during the contact process. Thus, they represent the contact force by the pure elastic Hertz's law combined with a nonlinear viscoelastic element expressed as

$$F_{\mathrm{N}} = K\delta^{n} + \chi\delta^{n}\dot{\delta} \tag{28}$$

where the parameter χ is called hysteresis damping factor that can be written as

$$\chi = \frac{3(1-c_r)}{2}\frac{K}{\dot{\delta}^{(-)}} \tag{29}$$

in which K is the contact stiffness parameter given by Eqs. (18) and (19), c_{r} denotes the coefficient of restitution and $\dot{\delta}^{(-)}$ represents the initial impact velocity. After some basic mathematical manipulation, the expression for the Hunt and Crossley contact force model can be written as follows

$$F_{\mathrm{N}} = K\delta^{n}\left[1 + \frac{3(1-c_{\mathrm{r}})}{2}\frac{\dot{\delta}}{\dot{\delta}^{(-)}}\right] \tag{30}$$

Besides the Hunt and Crossley approach is valid for direct central and frictionless contact, it has been used by many researchers because of its simplicity and straightforward to implement [9,128–130]. For instance, Guess et al. [131] employed the Hunt and Crossley formulation to successfully model the interaction between tibia, femur and menisci in a global three-dimensional multibody knee model. Due to the difficulty in defining the stiffness and damping coefficients of the contacting surfaces, these authors considered the stiffness and damping as design variables in an optimization process to match with the data obtained from a finite element model. Finally, it must be noted that the Hunt and Crossley contact force model is appropriate for contact cases in which the coefficient of restitution is high, at it was also demonstrated by Marhefka and Orin [24], Gonthier et al. [35] and Papetti et al. [132].

The use of the contact law given by Eq. (30) to the impact of two externally spheres implies the outcome illustrated in Fig. 4, where the contact force, the indentation, the force–indentation relation and the phase portrait are presented. The impact scenario is the same as in the example described for the pure elastic model given by Hertz's law presented in the previous section. A contact stiffness parameter of 5.5×10^{9} N/m$^{3/2}$ and a coefficient of restitution equal 0.7 have been considered for the calculations. From the plots of Fig. 4a it can be observed that the compression and restitution phases of the contact process are not equal due to the differences in the energy dissipation that occurs during these two phases. This fact is clear and visible in the non-symmetrical nature of the contact force curve. The energy dissipated during the contact process is associated with the hysteresis loop of the force–indentation diagram of Fig. 4b. The differences between the Hertz's law and Hunt and Crossley model can be observed in the plots of Fig. 4b and c. Fig. 4 shows the continuous nature of the contact forces, which build up from zero upon impact and smoothly return to zero upon separation. It is also visible that the forces developed in the contact process are always positive. Finally, it should be mentioned that with this

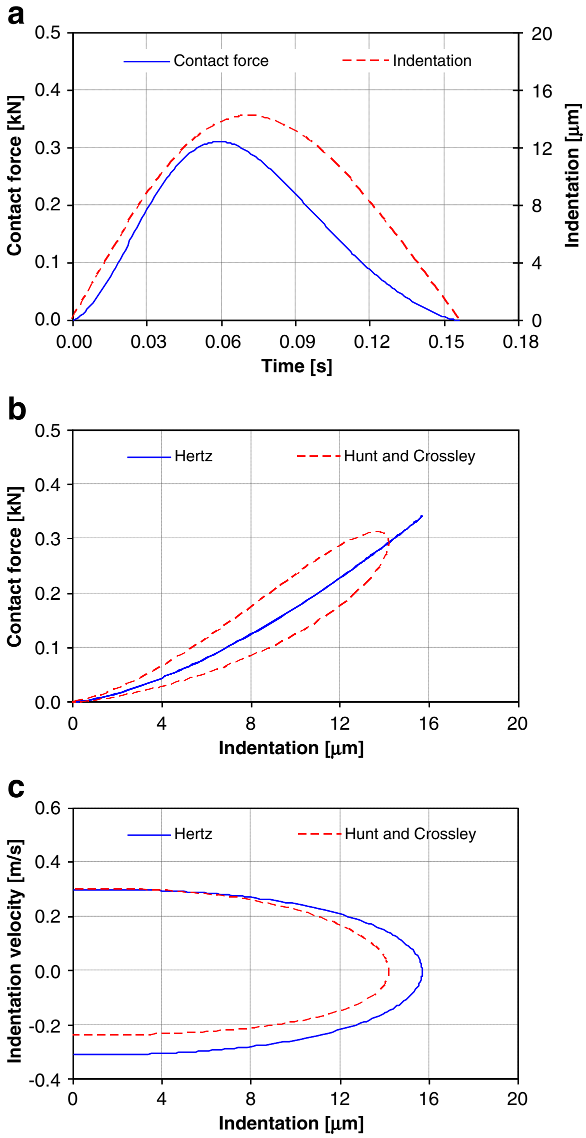

Fig. 4. Externally colliding spheres modeled by Hertz, and Hunt and Crossley contact force model: (a) contact force and indentation versus time; (b) force–indentation relation; (c) phase portrait.

contact force model, the energy dissipated during the contact is related to material damping of the contacting bodies. In this model the damping term is expressed as a function of indentation, which sounds reasonable from physical point of view.

A different formulation to account for the loss of energy in contact–impact events that has the coefficient of restitution as main parameter was presented by Herbert and McWhannell [133]. In this model, the authors combined the dynamic equations of motion of the impacting bodies with the Hunt and Crossley contact force model, being the hysteresis damping factor written as

$$\chi = \frac{6(1-c_{\mathrm{r}})}{\left[(2c_{\mathrm{r}}-1)^2+3\right]}\frac{K}{\dot{\delta}^{(-)}} \tag{31}$$

and the corresponding contact force expression is given by

$$F_{\mathrm{N}} = K\delta^n\left[1+\frac{6(1-c_{\mathrm{r}})}{\left[(2c_{\mathrm{r}}-1)^2+3\right]}\frac{\dot{\delta}}{\dot{\delta}^{(-)}}\right] \tag{32}$$

This approach can be considered as a refinement of the Hunt and Crossley contact force model. According to Herbert and McWhannell, the hysteresis loop predicted by Eqs. (30) and (32) differs by 1.5% [133]. The contact model given by Eq. (32) has been considered and applied by few researchers only, namely in the works by Yang and Sun [103] and Sarkar et al. [134] in the study of backlash effects in geared mechanisms.

Lee and Wang [45] proposed a new hysteresis damping factor that is quite similar to the one presented by Hunt and Crossley. Their main concern was to satisfy the expected hysteresis boundary conditions, that is, zero damping force at zero and maximum relative indentation of contact. Lee and Wang developed their work in the context of dynamic modeling and analysis of mechanisms with intermittent motion, being the hysteresis damping factor given by

$$\chi = \frac{3(1-c_r)}{4}\frac{K}{\dot{\delta}^{(-)}} \tag{33}$$

which results in the following expression for the contact force

$$F_N = K\delta^n\left[1 + \frac{3(1-c_r)}{4}\frac{\dot{\delta}}{\dot{\delta}^{(-)}}\right] \tag{34}$$

Besides its simplicity and similarities with the contact force model developed by Hunt and Crossley, the approach proposed by Lee and Wang is not very popular in multibody system contact problems.

Fig. 5 shows the force–indentation diagram and the phase portrait for the two externally impacting spheres considered in the example presented above, when the Hertz, Hunt and Crossley, Herbert and McWhannell, and Lee and Wang contact force models are utilized. It can be observed that the Hunt and Crossley approach gives force profile between the other two dissipative models. The Lee and Wang force model produces higher impact force magnitude due to the fact that less energy is dissipated in the impact. Furthermore, it can be concluded that the Herbert and McWhannell approach dissipates a larger amount of energy, visible in the larger hysteresis loop of the force–indentation curve of Fig. 5a, and also in the lower post-impact velocity seen in Fig. 5b.

One of the most popular and frequently contact force models used in multibody systems with contact–impact events is due to Lankarani and Nikravesh [34]. They obtained an expression for the hysteresis damping factor by relating the kinetic energy loss by the impacting bodies to the energy dissipated in the system due to internal damping. Considering the kinetic energies before and after impact, the amount of energy loss can be expressed as a function of the coefficient of restitution and initial impact velocity as

$$\Delta E = \frac{1}{2}m\dot{\delta}^{(-)^2}\left(1-c_r^2\right) \tag{35}$$

where m is the equivalent mass.

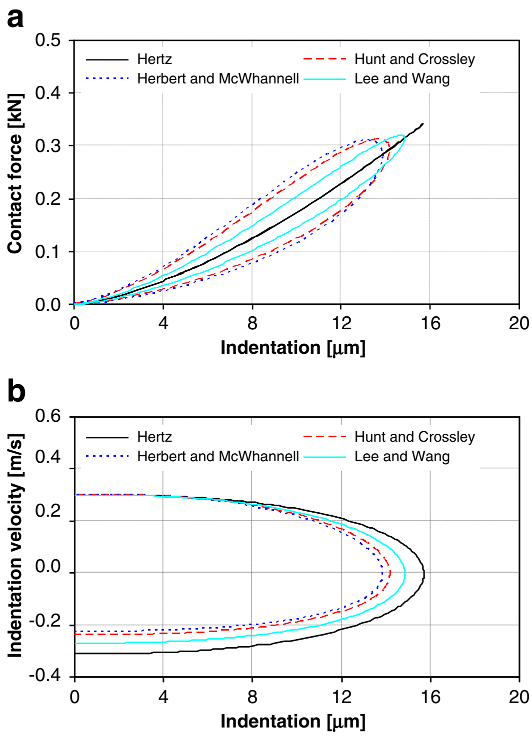

Fig. 5. Externally colliding spheres modeled by Hertz, Hunt and Crossley, Herbert and McWhannell, and Lee and Wang contact force models: (a) force–indentation relation; (b) phase portrait.

The energy loss can also be evaluated the integration of the contact force around the hysteresis loop. Assuming that the damping force characteristics during the compression and restitution phases are the same, it can be seen that [34]

$$\Delta E \simeq \frac{2}{3}\frac{\chi}{K} m \dot{\delta}^{(-)^3} \tag{36}$$

Thus, after substituting Eq. (35) in Eq. (36) an expression for the hysteresis damping factor is obtained as

$$\chi = \frac{3\left(1-c_\mathrm{r}^2\right)}{4}\frac{K}{\dot{\delta}^{(-)}} \tag{37}$$

which is a quadratic function of the coefficient of restitution.

Introducing now Eq. (37) into Eq. (28) results the continuous contact force model due to Lankarani and Nikravesh written here as

$$F_\mathrm{N} = K\delta^n\left[1+\frac{3\left(1-c_\mathrm{r}^2\right)}{4}\frac{\dot{\delta}}{\dot{\delta}^{(-)}}\right] \tag{38}$$

This contact force model is satisfactory for general mechanical contacts, in particular for the cases in which the energy dissipated during the contact is relatively small when compared to the maximum absorbed elastic energy. That is, Eq. (38) is mainly valid for the values of the coefficient of restitution close to unity [34]. Shivaswamy [135] demonstrated that at low impact velocities, the energy dissipation due to internal damping is the main contributor to energy loss. Since its publication, the Lankarani and Nikravesh contact force model has been utilized by numerous authors in different domains [136–141]. In a later paper, Lankarani and Nikravesh [97] extended their original work to include the plastic or permanent deformations that takes place at higher impact velocities.

The contact force models presented above, known as point contact models, are adequate for the cases where the area of contact is small when compared to the dimensions of the contacting bodies, that is, the contact is considered to occur at a single point. Therefore, in the situations of large contact areas, such as those associated with nonconformal contacts, a more superior model is required. In line with this concern, Gonthier and his co-workers [35] developed a volumetric contact force model for multibody dynamics in which the hysteresis damping factor is given by

$$\chi = \frac{d}{c_\mathrm{r}}\frac{K}{\dot{\delta}^{(-)}} \tag{39}$$

where the dimensionless factor d is defined as

$$1+\frac{d/c_\mathrm{r}}{1-d} = e^{d\left(1+1/c_\mathrm{r}\right)} \tag{40}$$

which can be approximated by

$$d \approx 1-c_\mathrm{r}^2 \tag{41}$$

and, finally, the Gonthier et al. force model can be written as

$$F_\mathrm{N} = K\delta^n\left[1+\frac{1-c_\mathrm{r}^2}{c_\mathrm{r}}\frac{\dot{\delta}}{\dot{\delta}^{(-)}}\right] \tag{42}$$

It should be mentioned that this approach gives the exact solution of the dynamic contact problem when Eq. (40) is considered, in contrast with the contact force models presented above that are approximate solutions base on different simplifications and assumptions. Moreover, by analyzing Eq. (39), it can be concluded that for a perfectly elastic contact, i.e. $c_\mathrm{r} = 1$, the hysteresis damping factor assumes a zero value, while for a purely inelastic contact, i.e. $c_\mathrm{r} = 0$, the hysteresis damping factor is infinite, which is reasonable from the physical point of view. This analysis is not true for the hysteresis damping factors given by Eqs. (29), (31), (33) and (37), in which this parameter does not assume an infinite value for null coefficient of restitution, as it would be expected. For high values of the coefficient of restitution with the Gonthier et al. force model, the compression and restitution phases are essentially symmetric. In sharp contrast, for low values of the coefficient of restitution, most of the energy is dissipated in the compression phase and the hysteresis loop is nonsymmetric [35].

The contact force model given Eq. (42) is often explicitly expressed as a function of the volume of interference and the contact volumetric stiffness. In this case, the unit for the force is per unit volume. With this approach, a new difficulty arises, which deals with the evaluation of the volumetric stiffness parameter. This particular issue has been recent object of theoretical and experimental investigations at the University of Waterloo [142,143].

More recently, Zhiying and Qishao [144] described a contact force in which the hysteresis damping factor is given by

$$\chi = \frac{3\left(1-c_{\mathrm{r}}^{2}\right)e^{2(1-c_{\mathrm{r}})}}{4}\frac{K}{\dot{\delta}^{(-)}} \tag{43}$$

and the force is expressed as

$$F_{\mathrm{N}} = K\delta^{n}\left[1+\frac{3\left(1-c_{\mathrm{r}}^{2}\right)e^{2(1-c_{\mathrm{r}})}}{4}\frac{\dot{\delta}}{\dot{\delta}^{(-)}}\right] \tag{44}$$

The work by Zhiying and Qishao, published in Chinese language, was developed in the context of impact analysis which purpose was to derive a relation between the coefficient of restitution, the contact parameters and the energy dissipated in the contact process.

Another contact force model recently published was due to Flores and his co-authors [36] that was developed with the foundation of the Hertz contact theory together with a hysteresis damping parameter that accommodates the loss of energy during the contact process. For this purpose, an expression for the hysteresis damping factor was derived by evaluating the kinetic energy dissipated in the system due to internal damping. On one hand, the kinetic energy loss can be expressed as a function of the coefficient of restitution and initial impact velocity and is given by Eq. (35). On the other hand, the energy dissipated during the contact process can be determined by integrating the contact force around the hysteresis loop. Flores et al. [36] considered that the energy dissipated is due internal damping and was evaluated by modeling the contact event as a dynamic single degree-of-freedom system, yielding

$$\Delta E = \frac{1}{4}\chi(1-c_{\mathrm{r}})\dot{\delta}^{(-)}\delta_{\max}^{\frac{5}{2}} \tag{45}$$

where $\delta_{\max}$ refers to the maximum indentation. Thus, substituting Eq. (45) in Eq. (35) and taking into account the linear momentum balance yields the following expression for the hysteresis damping factor as

$$\chi = \frac{8(1-c_{\mathrm{r}})}{5c_{\mathrm{r}}}\frac{K}{\dot{\delta}^{(-)}} \tag{46}$$

and, hence the contact force model is expressed as

$$F_{\mathrm{N}} = K\delta^{n}\left[1+\frac{8(1-c_{r})}{5c_{\mathrm{r}}}\frac{\dot{\delta}}{\dot{\delta}^{(-)}}\right] \tag{47}$$

It must be stated that this contact force model was developed for situations between very elastic and inelastic contacting materials, being the outcomes similar to those obtained with the Gonthier et al. force model given by Eq. (42).

Fig. 6 depicts the force–indentation relation and the phase portrait for the two impacting spheres described above, when the contact is model with the Hertz, Hunt and Crossley, Lankarani and Nikravesh, Gonthier et al., Zhiying and Qishao, and Flores et al. formulations. From the plots it can be observed that the outcomes of the Hunt and Crossley approach and Lankarani and Nikravesh force model do not differ in a significant manner. This fact is not surprising because these two models were developed taking into account the similar simplifying premises. In addition, the results obtained with the Gonthier et al., Zhiying and Qishao, and Flores et al. force models present a quite close evolution, in which the compression and restitution phases of the contact process are not equal to each other due to the differences in the energy dissipation between these two phases. This fact is visible by observing the non-symmetrical nature of the contact force–indentation plots.

With the purpose to better understand what are the main differences between the dissipative contact force models presented above, the evolution of the hysteresis damping factor for all the entire range of the coefficient of restitution is analyzed, as Fig. 7 illustrates. In order to keep the analysis simple, the contact stiffness parameter and the initial impact velocity are equal to each other and equal to unity. By observing the plots of Fig. 7, it can be concluded that the contact force models exhibit a similar behavior for high values of coefficient of restitution. Furthermore, the Hunt and Crossley, Herbert and McWhannell, Lee and Wang, and Lankarani and Nikravesh formulations do not work adequately for low values of the coefficient of restitution. In particular, the Lee and Wang approach the one that dissipated less amount of energy during the contact process. In turn, the Zhiying and Qishao contact force model presents a superior response mainly for low values of the coefficient of restitution. The force approaches due to Gonthier et al. and Flores et al. have a similar behavior and for low values of the coefficient of restitution the hysteresis damping factor increases asymptotically with the decrease of the coefficient of restitution, which means that they can perform well for perfectly inelastic contacts. Moreover, it must be highlighted that for moderate and high values of the coefficient of restitution, the Gonthier et al., the Zhiying and Qishao, and the Flores et al. force models present a very close response. This fact is true for coefficients of restitution higher than 0.5, as it can be observed in the diagrams plotted in Fig. 7.

Finally, it must be stated that there are other contact force models candidate to be utilized in multibody system contact problems and some more insights can be obtained from works that have been developed independently of those described in the present work. In particular, the interested reader can find relevant information on the impact between spheres in the publications by

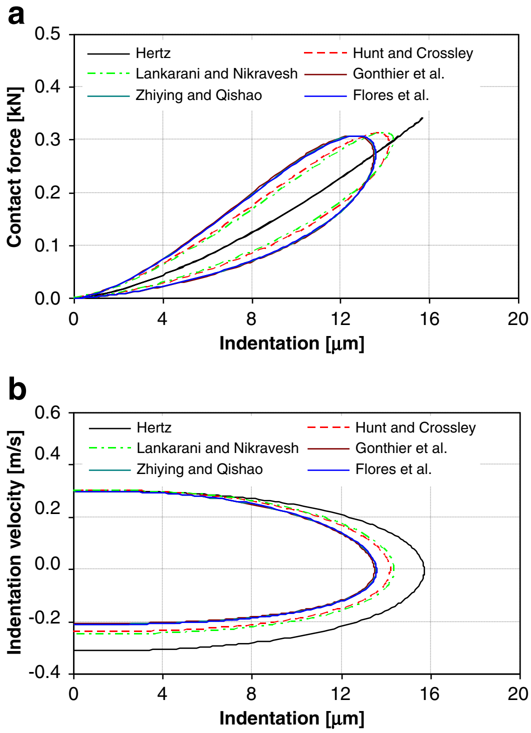

Fig. 6. Externally colliding spheres modeled by Hertz, Hunt and Crossley, Lankarani and Nikravesh, Gonthier et al., Zhiying and Qishao, and Flores et al. contact force models: (a) force–indentation relation; (b) phase portrait.

Yigit et al. [145,146], Thornton [147], Gugan [148], Falcon et al. [149], Rigaud and Perret-Liaudet [150], Kuwabara and Kono [151], Minamoto and Kawamura [152], Kagami et al. [153], Pust and Peterka [154], Vu-Quoc et al. [155,156], Burgin and Aspden [157], Bordbar and Hyppänen [158], Yoshioka [159], Villaggio [160], Ramírez et al. [161], Wu et al. [162,163], Shi and Polycarpou [164], Tatara and Moriwaki [165], Tatara [166].

6. Demonstrative examples of application

A planar slider-crank mechanism experiencing two frictionless impacts with an external free sliding block is a classical contact–impact problem selected as a first example of application. This multibody system is considered here to study the influence of the use of different compliant contact force models on the simulation of the dynamic response of multibody systems. Fig. 8 shows a generic configuration of the system which consists of five rigid bodies representing the slider-crank mechanism and the free sliding block. The body numbers and their corresponding coordinate systems are also shown in Fig. 8. The system is kinematically constrained through the constraint equations associated with the three revolute joints and one translational joint, making a multibody model with a total of two degrees-of-freedom. The slider-crank mechanism is initialized with a crank angular velocity of 150 rad/s counter clockwise. Furthermore, the remaining initial conditions, necessary to start the dynamic simulations, are obtained from a previous kinematic analysis of the slider-crank mechanism. At the start of the dynamic analysis, the crank and

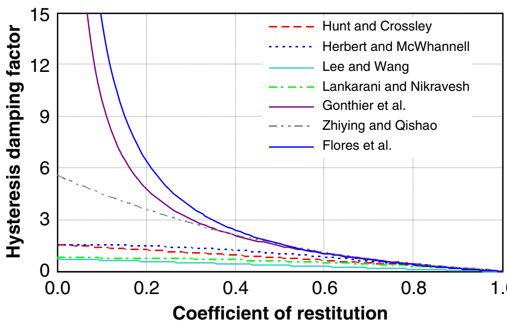

Fig. 7. Evolution of the hysteresis damping factor as function of the coefficient of restitution for all of the dissipative contact force models.

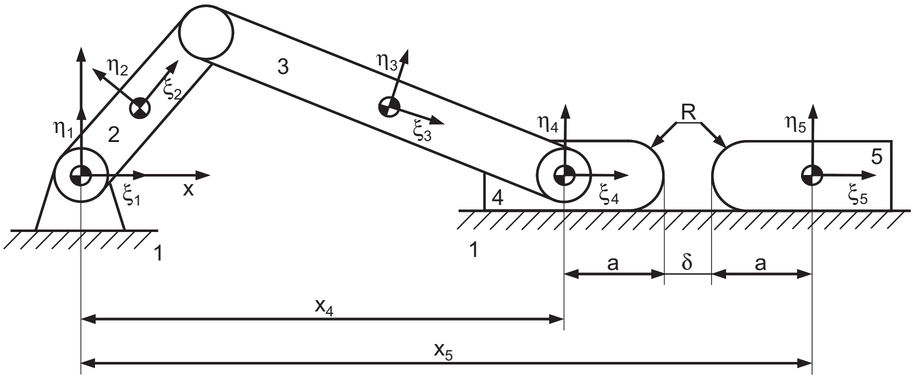

Fig. 8. Multibody system composed by a slider-crank mechanism and a free sliding block.

connecting-rod links are aligned in the x direction that corresponds to the dead point. Initially, the free sliding block is driven at a constant linear velocity equal to 15 m/s to the left. The initial position of the sliding block is located at x coordinate equal to 0.914 m. This multibody system is acted upon by gravitational force only which is taken as acting in the negative y direction, being the system defined as moving in the vertical plane. The set of data considered to build the multibody model used to perform the dynamic simulations is listed in Table 1. The integration process is performed by using a predictor-corrector algorithm with both variable step size and order so that smaller step sizes during the contact events can automatically be adjusted for. In turn, with the purpose to keep under control the constraints violation, the dynamic equations of motion are solved by employing the Baumgarte stabilization technique.

The contact surfaces of the sliding bodies have spherical shapes with radius equal to 8.5 mm and the contact stiffness parameter is evaluated as 9.5×10^9 N/m$^{3/2}$. The value of the restitution coefficient used in the simulations is equal to 0.7. The geometric condition that allows for the evaluation of the relative indentation between the sliding bodies can be written as

$$\delta = x_5 - x_4 - 2a \tag{48}$$

where x_5 and x_4 represent the x coordinate of the sliding bodies and the dimension a, shown in Fig. 8, is equal to 16.93 mm.

At some instances, due to the system's initial configuration and its dynamic behavior, the constrained slider impacts twice with free sliding block. In the present study, the performance of this multibody system is quantified by the plots of the position of the free sliding block and the velocity of the constrained slider. In addition, the force–indentation relation for the two impacts are also plotted and analyzed. For this purpose, seven different compliant contact force models are utilized namely, Hunt and Crossley, Herbert and McWhannell, Lee and Wang, Lankarani and Nikravesh, Gonthier et al., Zhiying and Qishao, Flores et al. approaches, which were briefly described in the previous section.

The time history of the position of the free sliding block and the velocity of the constrained slider are represented in the plots of Fig. 9. The two impacts between the sliders that occur during the dynamic simulation are visible by the discontinuities of those plots. By analyzing the curves plotted in Fig. 9, it can be observed that the contact force model proposed by Lee and Wang produces impacts with higher rebounds, because the less amount of energy dissipated in the two contact events. Furthermore, it is noteworthy that the Gonthier et al., Zhiying and Qishao, and Flores et al. force models exhibit a very similar behavior, for which rebounds are of less magnitude when compared with the remaining formulations. This phenomenon is quite visible in both position and velocity diagrams of Fig. 9. Finally, as it was expected, the Lankarani and Nikravesh, Hunt and Crossley, the Herbert and McWhannell approaches present an intermediate response, and the Herbert and McWhannell force model the most dissipative one among these last three approaches.

Fig. 10 shows the force–indentation plots for the two impacts between the slider bodies. Again, it is observed that the Lee and Wang model is the one that dissipates less energy visible in the smaller hysteresis loop. In turn, the Gonthier et al., Zhiying and Qishao, and Flores et al. force models dissipate more energy, exhibiting larger hysteresis loops. As a consequence, the rebounding velocity is lower when compared to the other force models. This analysis is valid for both impacts, as it can be seen in Fig. 10a and b. Finally, the same conclusion that was drawn above can be achieved here too, that is for the Lankarani and Nikravesh, Hunt and

Table 1
Geometrical and inertial properties of the slider-crank mechanism and free sliding block.

Body	Length [m]	Mass [kg]	Moment of inertia [kg m^2]
Crank	0.153	0.038	7.4×10^{-5}
Connecting rod	0.306	0.076	5.9×10^{-5}
Slider	-	0.038	1.8×10^{-6}
Free block	-	0.190	2.7×10^{-5}

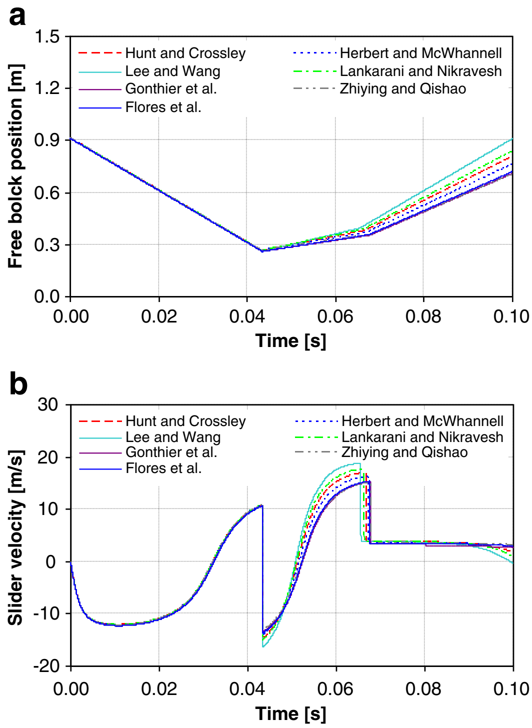

Fig. 9. (a) Position of the free sliding block; (b) velocity of the constrained slider.

Crossley, and Herbert and McWhannell approaches. In short, the contact force models can be grouped into two main classes, one for the higher dissipative approaches that comprises the Gonthier et al., the Zhiying and Qishao, and Flores et al. force models, and another one for the remaining formulations.

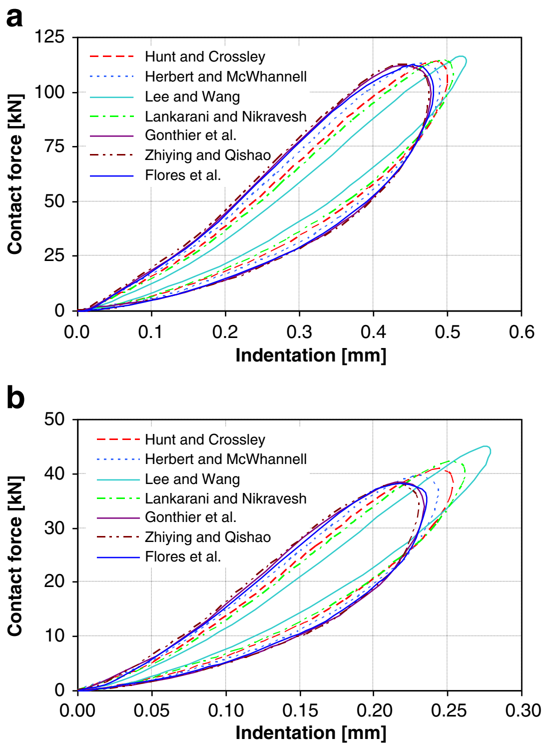

Fig. 10. Force–indentation relation for the two impacts between the slider bodies: (a) first impact; (b) second impact.

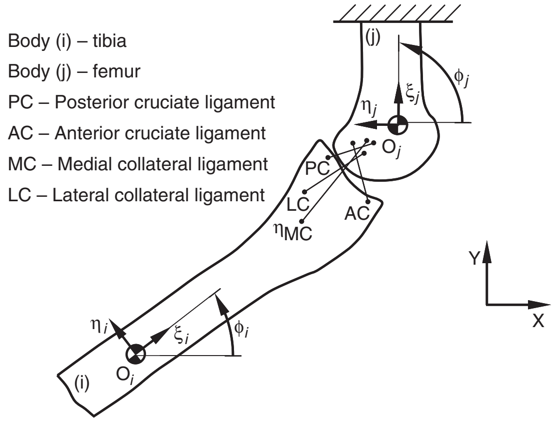

Fig. 11. Knee joint including the femur and tibia elements and the four primary ligaments.

As a second example of application, a two-dimensional knee model that experiences contact–impact events is considered [167]. Fig. 11 shows two bodies i and j which represent the tibia and femur, respectively. Body-fixed coordinate systems $\xi\eta$ are attached to each body, while xy coordinate frame represents the global coordinate system. The origin of the femur coordinate system is located at the intercondylar notch, while the origin of the tibia coordinate system is located at the center of mass of the tibia, with the local ξ-axes directed proximally and η-axes directed posteriorly. These origin points are represented by points O_i and O_j. The angles of rotation of the local coordinate systems of bodies i and j, relative to the global system, are denoted by ϕ_i and ϕ_j, respectively.

The Cartesian coordinates of centers of mass and inertia properties of the femur and tibia are listed in Table 2, which are assigned to the segments on values derived for a similar model of a 76 kg, 1.8 m tall male by Yamaguchi [168].

In the present work, the femur and tibia elements are modeled as two contacting bodies, while their dynamics is controlled by contact forces. The knee joint elements are considered to be rigid and describe a general planar motion in the sagittal plane. The femur is considered to be stationary, while the tibia rolls and slides in relation to the femur profile. The femur and tibia are connected by four nonlinear elastic springs in order to represent the knee joint ligaments, as illustrated in Fig. 11. The following force–elongation relation is utilized for each ligament

$$F_l = \begin{cases} k_l\left(l_l - l_l^0\right)^2 & \text{if } l_l > l_l^0 \\ 0 & \text{if } l_l \le l_l^0 \end{cases} \tag{49}$$

where k_l is the ligament stiffness, l_l and l_l^0 are the current and the unstrained lengths of the ligaments, respectively. The unstrained lengths of the four ligaments are adopted from the Moeinzadeh et al. work [169]. The initial position of the tibia at 54.8 degrees of knee flexion is selected as it corresponds to a particular position where the ligaments are in a relatively relaxed condition, and therefore the knee contact forces can be neglected. The local coordinates of the ligament insertion points, as well as their physical properties (unstrained length and stiffness) are listed in Table 3.

Based on medical imaging techniques, the femur and tibia profiles in the sagittal plane are extracted and used to define the interface geometric conditions for contact. The general contact procedure presented in Section 3 is utilized to deal with the

Table 2
Cartesian coordinates and inertia properties of the femur and tibia bodies.

Body name	x [m]	y [m]	ϕ [°]	Mass [kg]	Moment of inertia [kg m^2]
Femur	0.0000	0.0000	90.00	7.580	0.1260
Tibia	−0.2016	−0.1749	35.21	3.750	0.0165

Table 3
Local coordinates of the insertion points and physical properties of the ligaments.

Ligament	AC	PC	MC	LC
ξ_f^l[m]	−0.0330	−0.0190	−0.0230	−0.0250
η_f^l[m]	−0.0170	−0.0140	−0.0140	−0.0190
ξ_t^l[m]	0.2130	0.2100	0.1630	0.1780
η_t^l[m]	−0.0090	0.0350	0.0080	0.0250
l_l^0[m]	0.0438	0.0332	0.0784	0.0562
k_l[kN/m^2]	35000	30000	15000	15000

contact problem within this example of application. When a contact is detected, a continuous nonlinear contact force law is applied which calculates the contact forces developed at the interface as a function of the relative indentation between the two bodies. The articular cartilages of the knee are modeled as linear elastic and isotropic material with an elastic modulus of $E=5$ MPa and a Poisson's ratio of $\nu=0.46$ [170]. The value of the restitution coefficient used in the simulations is equal to 0.6 [157]. The forces produced in the ligaments, together with the contact forces, are introduced into the system's equations of motion as generalized forces. Furthermore, an external applied force, F_e, is applied on the system, as Fig. 11 shows, being expressed by

$$F_{\mathrm{e}} = Ae^{-4.73\left(\frac{t}{t_{\mathrm{d}}}\right)^2}\sin\left(\frac{\pi t}{t_{\mathrm{d}}}\right) \tag{50}$$

which is an exponentially decaying sinusoidal pulsed function of duration t_d and with an amplitude A. The simulations are performed for 0.4 s of duration with a time step of 1E-4s, and with amplitude A equal to 50 N. In order to keep the analysis simple, only three contact force models are considered in the dynamic simulations of the knee system, namely the Hertz, Lankarani and Nikravesh and Flores et al. approaches. By observing the plots of Fig. 12, it can be observed that Hertz model causes oscillations in the force–indentation diagram due to the pure elastic nature of this formulation. In contrast, the Lankarani and Nikravesh and Flores et al. models present a smoother behavior. In particular, when the system is modeled with the Flores et al. model it produces higher contact forces with almost no oscillations, at is can be observed in Fig. 12a. Because the knee model experiences contacts that take place with low impact velocities, the contact is essentially continuous, as it is visible in the plots of Fig. 12b.

7. Concluding remarks

A general and comprehensive study of some of the most relevant compliant contact force models for multibody systems dynamics has been presented in this work. In the sequel of this process, the main characteristics, advantages and limitations of the pure elastic and dissipative contact force models were also analyzed. Furthermore, the fundamental formalisms available in the literature to model multibody systems and the generalized contact kinematics were revisited. Finally, two simple planar multibody systems that include contact–impact scenarios were considered as examples of application to demonstrate the similarities of and differences between the contact force models used throughout this work.

There is no doubt that the biggest landmark in contact mechanics was the work of Hertz for static elastic contacts. The Hertzian contact approach is based on the theory of elasticity and still remains the foundation for elastic and dissipative contact force models available in the literature. In a simple manner, the dissipative models extended the Hertz's law to include, a damping term that

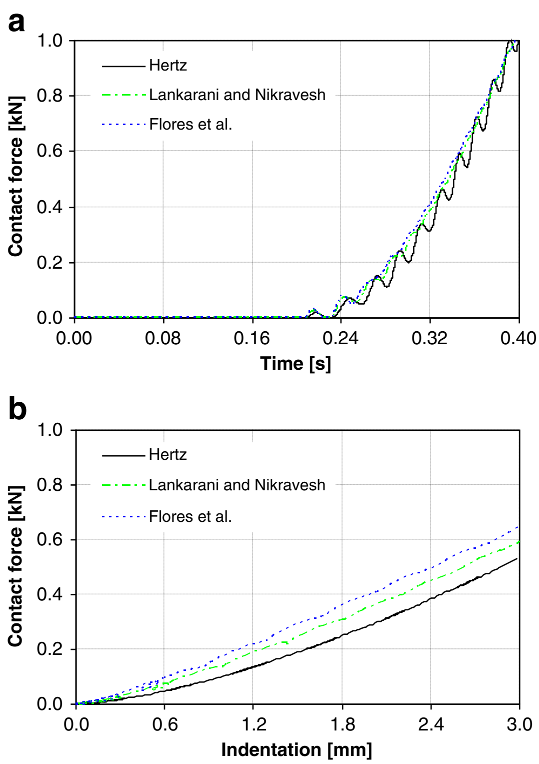

Fig. 12. Knee contact modeled by Hertz, Hunt and Crossley, Lankarani and Nikravesh, Gonthier et al., and Flores et al. contact force models (a) contact force versus time; (b) force–indentation relation.

accommodates some amount of energy loss during the impact process for low to moderate impact velocities. This dissipative term is expressed as function of the coefficient of restitution. It was shown in this work that several authors have proposed different relations between the coefficient of restitution and energy dissipation. Some of them are approximations, such as the Hunt and Crossley model, while other relations present an exact solution of the dynamic equations of motion for an impact between two bodies, such as the model proposed by Gonthier et al. Nevertheless, all contact force models have been correctly developed from the scientific point of view. The compliant contact force models studied in this work exhibit some interesting features. In the first place, they consider the geometric, kinematic and material properties of the contacting surfaces, which is of paramount importance in the contact dynamic performance of the systems. These models are also computationally efficient and straightforward to implement in general-purpose multibody systems codes. In addition, the contact force models can easily incorporate friction models.

The dissipative formulations described and compared in this work can be distinguished by different damping force components that augmented the Hertz's law. For high values of the coefficient of restitution, the contact force models exhibit a quite similar behaviour, namely when this coefficient is close to unity that represents very elastic contacts. In sharp contrast, for moderate or low coefficients of restitution, the Gonthier et al., Zhiying and Qishao, and Flores et al. approaches present a superior performance, when compared to other models. In these three models, the increase in damping reduces the indentation because there is less energy to store in the contact process. This particular aspect plays a crucial role in the prediction of the dynamic response of multibody systems and has consequences in the analysis and design process of mechanical systems. Thus, in order to correctly model, analyze and simulate multibody systems in general, appropriate contact force models must be adopted.

Acknowledgments

The authors would like to thank the Portuguese Foundation for Science and Technology (FCT) for the support given through projects DACHOR—Multibody Dynamics and Control of Hybrid Active Orthoses (MIT-Pt/BSHHMS/0042/2008) and BIOJOINTS—Development of advanced biological joint models for human locomotion biomechanics (PTDC/EME-PME/099764/2008). The first and second authors express their gratitude to FCT for the PhD grants SFRH/BD/40164/2007 and SFRH/BD/64477/2009, respectively.

References

[1] H.-T. Pham, D.-A. Wang, A constant-force bistable mechanism for force regulation and overload protection, Mechanism and Machine Theory 46 (2011) 899–909.
[2] I. González-Péréz, J.L. Iserte, A. Fuentes, Implementation of Hertz theory and validation of a finite element model for stress analysis of gear drives with localized bearing contact, Mechanism and Machine Theory 46 (2011) 765–783.
[3] D. Dopico, A. Luaces, M. Gonzalez, J. Cuadrado, Dealing with multiple contacts in a human-in-the-loop application, Multibody System Dynamics 25 (2011) 167–183.
[4] S.H. Zhu, S. Zwiebel, G. Bernhardt, A theoretical formula for calculating damping in the impact of two bodies in a multibody system, Proceedings of the Institution of Mechanical Engineers, Part C: Journal of Mechanical Engineering Science 213 (1999) 211–216.
[5] J. Ambrósio, P. Veríssimo, Improved bushing models for general multibody systems and vehicle dynamics, Multibody System Dynamics 22 (2009) 341–365.
[6] S. Ebrahimi, G. Lari, Identification of compliant contact force parameters in multibody systems based on the neural network approach, in: J.C. Samin, P. Fisette (Eds.), Proceedings of the Multibody Dynamics 2011, ECCOMAS Thematic Conference, July 4-7 2011, Brussels, Belgium, 9 pp.
[7] K.H. Hunt, F.R.E. Crossley, Coefficient of restitution interpreted as damping in vibroimpact, Journal of Applied Mechanics 7 (1975) 440–445.
[8] P. Dietl, J. Wensing, G.C. van Nijen, Rolling bearing damping for dynamic analysis of multi-body systems—experimental and theoretical results, Proceedings of the Institution of Mechanical Engineers, Part K: Journal of Multi-body Dynamics 214 (2000) 33–43.
[9] P. Moreira, M. Silva, P. Flores, A biomechanical multibody foot model for forward dynamic analysis, Proceedings of the 1st Joint International Conference on Multibody Dynamics, Lappeenranta, Finland, May 25-27 2010, 10 pp.
[10] P. Flores, Modeling and simulation of wear in revolute clearance joints in multibody systems, Mechanism and Machine Theory 44 (2009) 1211–1222.
[11] Q. Tian, Y. Zhang, L. Chen, P. Flores, Dynamics of spatial flexible multibody systems with clearance and lubricated spherical joints, Computers and Structures 87 (2009) 913–929.
[12] D. Mihai, D.G. Beale, Dynamic analysis of a flexible linkage mechanism with cracks and clearance, Mechanism and Machine Theory 45 (2010) 1909–1923.
[13] T.K. Naskar, S. Acharyya, Measuring cam-follower performance, Mechanism and Machine Theory 45 (2010) 678–691.
[14] J. Pombo, J. Ambrósio, M. Pereira, R. Lewis, R. Dwyer-Joyce, C. Ariaudo, N. Kuka, A study on wear evaluation of railway wheels based on multibody dynamics and wear computation, Multibody System Dynamics 24 (2010) 347–366.
[15] P. Flores, R. Leine, C. Glocker, Modeling and analysis of planar rigid multibody systems with translational clearance joints based on the non-smooth dynamics approach, Multibody System Dynamics 23 (2010) 165–190.
[16] K.D. Bhalerao, K.S. Anderson, Modeling intermittent contact for flexible multibody systems, Nonlinear Dynamics 60 (2010) 63–79.
[17] F. Pfeiffer, On non-smooth dynamics, Meccanica 43 (2008) 533–554.
[18] C. Glocker, Formulation of spatial contact situations in rigid multibody systems, Computer Methods in Applied Mechanics and Engineering 177 (1999) 199–214.
[19] A. Lichtenberg, M. Liebermann, Regular and Chaotic Dynamics, Springer-Verlag, New York, 1992.
[20] K.L. Johnson, Contact Mechanics, Cambridge University Press, Cambridge, 1999.
[21] P. Flores, A parametric study on the dynamic response of planar multibody systems with multiple clearance joints, Nonlinear Dynamics 61 (2010) 633–653.
[22] P. Wriggers, Computational Contact Mechanics, Second Edition Springer-Verlag, Berlin, 2006.
[23] Y.-C. Lin, R.T. Haftka, N.V. Queipo, B.J. Fregly, Surrogate articular contact models for computationally efficient multibody dynamics simulations, Medical Engineering & Physics 32 (2010) 584–594.
[24] D.W. Marhefka, D.E. Orin, A compliant contact model with nonlinear damping for simulation of robotic systems, IEEE Transactions on Systems, Man and Cybernetics - Part A: Systems and Humans 29 (1999) 566–572.
[25] H.M. Lankarani, Canonical equations of motion and estimation of parameters in the analysis of impact problems, Ph.D. Dissertation, University of Arizona, Tucson, Arizona, 1988.
[26] F. Pfeiffer, C. Glocker, Multibody Dynamics with Unilateral Contacts, John Wiley & Sons, New York, 1996.
[27] B. Brogliato, A.A. Ten Dam, L. Paoli, F. Genot, M. Abadie, Numerical simulations of finite dimensional multibody nonsmooth mechanical systems, Applied Mechanics Reviews 55 (2002) 107–150.
[28] F. Pfeiffer, The idea of complementarity in multibody dynamics, Archive of Applied Mechanics 72 (2003) 807–816.

[29] Y.T. Wang, V. Kumar, Simulation of mechanical systems with multiple frictional contacts, Journal of Mechanical Design 116 (1994) 571–580.
[30] E. Pratt, A. Léger, M. Jean, About a stability conjecture concerning unilateral contact with friction, Nonlinear Dynamics 59 (2010) 73–94.
[31] A. Tasora, M. Anitescu, A convex complementarity approach for simulating large granular flows, Journal of Nonlinear and Computational Dynamics 5 (2010) 031004, 10 pages.
[32] P. Flores, J. Ambrósio, J.P. Claro, Dynamic analysis for planar multibody mechanical systems with lubricated joints, Multibody System Dynamics 12 (2004) 47–74.
[33] P. Flores, J.C.P. Claro, H.M. Lankarani, A comparative study on continuous contact force models for constrained multibody systems, in: J.C. Samin, P. Fisette (Eds.), Proceedings of the Multibody Dynamics 2011, ECCOMAS Thematic Conference, July 4-7 2011, Brussels, Belgium, 20 pp.
[34] H.M. Lankarani, P.E. Nikravesh, A contact force model with hysteresis damping for impact analysis of multibody systems, Journal of Mechanical Design 112 (1990) 369–376.
[35] Y. Gonthier, J. McPhee, C. Lange, J.-C. Piedboeuf, A regularized contact model with asymmetric damping and dwell-time dependent friction, Multibody System Dynamics 11 (2004) 209–233.
[36] P. Flores, M. Machado, M.T. Silva, J.M. Martins, On the continuous contact force models for soft materials in multibody dynamics, Multibody System Dynamics 25 (2011) 357–375.
[37] R.R. Ryan, ADAMS-Multibody system analysis software, Multibody systems handbook, Springer-Verlag, Berlin, 1990.
[38] R.C. Smith, E.J. Haug, DADS—Dynamic analysis and design system, Multibody Systems Handbook, Springer-Verlag, Berlin, 1990.
[39] Visual NASTRAN 4D, MSC Software, 2002.
[40] A.A. Shabana, Dynamics of Multibody Systems, John Wiley & Sons, New York, 1989.
[41] J. Choi, H.S. Ryu, C.W. Kim, J.H. Choi, An efficient and robust contact algorithm for a compliant contact force model between bodies of complex geometry, Multibody System Dynamics 23 (2010) 99–120.
[42] W.J. Stronge, Impact Mechanics, Cambridge University Press, Cambridge, 2000.
[43] W. Goldsmith, Impact—The Theory and Physical Behaviour of Colliding Solids, Edward Arnold Ltd., London, England, 1960.
[44] X. Zhang, L. Vu-Quoc, Modeling the dependence of the coefficient of restitution on the impact velocity in elasto-plastic collisions, International Journal of Impact Engineering 27 (2002) 317–341.
[45] T.W. Lee, A.C. Wang, On the dynamics of intermittent-motion mechanisms, Part 1: dynamic model and response, Journal of Mechanisms, Transmissions, and Automation in Design 105 (1983) 534–540.
[46] S.A.M. Najafabadi, J. Kövecses, J. Angeles, Generalization of the energetic coefficient of restitution for contacts in multibody systems, Journal of Nonlinear and Computational Dynamics 3 (2008) 0410081, 14 pages.
[47] R.L. Jackson, I. Green, D.B. Marghitu, Predicting the coefficient of restitution of impacting elastic-perfectly plastic spheres, Nonlinear Dynamics 60 (2010) 217–229.
[48] R. Seifried, W. Schiehlen, P. Eberhard, The role of the coefficient of restitution on impact problems in multi-body dynamics, Proceedings of the Institution of Mechanical Engineers, Part K: Journal of Multi-body Dynamics 224 (2010) 279–306.
[49] H. Hertz, Über die Berührung fester elastischer Körper, Journal reine und angewandte Mathematik 92 (1881) 156–171.
[50] W. Schiehlen, Multibody system dynamics: roots and perspectives, Multibody System Dynamics 1 (1997) 149–188.
[51] J. Wittenburg, Dynamics of Systems of Rigid Bodies, B.G. Teubner, Stuttgart, Germany, 1977.
[52] P. Nikravesh, Computer-Aided Analysis of Mechanical Systems, Prentice Hall, Englewood Cliffs, New Jersey, 1988.
[53] E.J. Haug, Computer-Aided Kinematics and Dynamics of Mechanical Systems—Volume I: Basic Methods, Allyn and Bacon, Boston, Massachusetts, 1989.
[54] R.L. Huston, Multibody Dynamics, Butterworth-Heinemann, Boston, Massachusetts, 1990.
[55] W. Schiehlen, Multibody Systems Handbook, Springer-Verlag, Berlin, Germany, 1990.
[56] P.E. Nikravesh, Planar Multibody Dynamics: Formulation, Programming, and Applications, CCR Press, London, 2008.
[57] W. Schiehlen, Computational aspects in multibody system dynamics, Computer Methods in Applied Mechanics and Engineering 90 (1990) 569–582.
[58] W. Schiehlen, Computational dynamics: theory and applications of multibody systems, European Journal of Mechanics A/Solids 25 (2006) 566–594.
[59] A.A. Shabana, Flexible multibody dynamics: review of past and recent developments, Multibody System Dynamics 1 (1997) 189–222.
[60] H. Rahnejat, Multi-body dynamics: historical evolution and application, Journal of Mechanical Engineering Science 214 (2000) 149–173.
[61] P. Eberhard, E. Schiehlen, Computational dynamics of multibody systems: history, formalisms, and applications, Journal of Computational and Nonlinear Dynamics 1 (2006) 3–12.
[62] J.G. Jalón, Twenty-five years of natural coordinates, Multibody System Dynamics 18 (2007) 15–33.
[63] P.E. Nikravesh, Newtonian-based methodologies in multi-body dynamics, Proceedings of the Institution of Mechanical Engineers, Part K: Journal of Multi-body Dynamics 222 (2008) 277–288.
[64] J.M. Jiménez, A. Avello, A. García-Alonso, J.G. Jálon, COMPAMM—a simple and efficient code for kinematic and dynamic numerical simulation of 3-D multi-body system with realistic graphics, in: W. Schiehlen (Ed.), Multibody Systems Handbook, Springer-Verlag, Berlin, 1990, pp. 285–304.
[65] W. Rulka, SIMPACK—a computer program for simulation of large motion multibody systems, in: W. Schiehlen (Ed.), Multibody Systems Handbook, Springer-Verlag, Berlin, 1990, pp. 265–284.
[66] W. Schiehlen, E. Kreuzer, Symbolic computational derivation of equations of motion, in: K. Magnus (Ed.), Dynamics of Multibody Systems, Springer, Berlin, 1978, pp. 290–305.
[67] J. Baumgarte, Stabilization of constraints and integrals of motion in dynamical systems, Computer Methods in Applied Mechanics and Engineering 1 (1972) 1–16.
[68] R.A. Wehage, E.J. Haug, Generalized coordinate partitioning for dimension reduction in analysis of constrained systems, Journal of Mechanical Design 104 (1982) 247–255.
[69] E. Bayo, J.G. Jálon, A.A. Serna, Modified Lagrangian formulation for the dynamic analysis of constrained mechanical systems, Computer Methods in Applied Mechanics and Engineering 71 (1988) 183–195.
[70] P. Flores, M. Machado, E. Seabra, M.T. Silva, A parametric study on the Baumgarte stabilization method for forward dynamics of constrained multibody systems, Journal of Computational and Nonlinear Dynamics 6 (1) (2011) 0110191–0110199.
[71] M.A. Neto, J. Ambrósio, Stabilization methods for the integration of DAE in the presence of redundant constraints, Multibody System Dynamics 10 (2003) 81–105.
[72] C.W. Gear, Numerical solution of differential-algebraic equations, IEEE Transactions on Circuit Theory CT-18 (1981) 89–95.
[73] P. Flores, MUBODYNA—A FORTRAN Program for Dynamic Analysis of Planar Multibody Systems, University of Minho, Guimarães, Portugal, 2010.
[74] W. Bu, Z. Liu, J. Tan, S. Gao, Detachment avoidance of joint elements of a robotic manipulator with clearances based on trajectory planning, Mechanism and Machine Theory 45 (2010) 925–940.
[75] J. Ambrósio, P. Veríssimo, Sensitivity of a vehicle ride to the suspension bushing characteristics, Journal of Mechanical Science and Technology 23 (2009) 1075–1082.
[76] M.P.T. Silva, J.A.C. Ambrósio, Kinematic data consistency in the inverse dynamic analysis of biomechanical systems, Multibody System Dynamics 8 (2002) 219–239.
[77] P. Flores, A methodology for quantifying the position errors due to manufacturing and assemble tolerances, Journal of Mechanical Engineering 57 (2011) 457–467.
[78] J. Ambrósio, Train kinematics for the design of railway vehicle components, Mechanism and Machine Theory 45 (2010) 1035–1049.
[79] J.A.C. Ambrósio, M.A. Neto, R.P. Leal, Optimization of complex flexible multibody systems with composite materials, Multibody System Dynamics 18 (2007) 117–144.
[80] P. Flores, J. Ambrósio, J.C.P. Claro, H.M. Lankarani, Kinematics and dynamics of multibody systems with imperfect joints: models and case studies, Lecture Notes in Applied and Computational Mechanics, Vol. 34, Springer, Berlin, 2008.
[81] D.T. Greenwood, Principles of Dynamics, Prentice Hall, Englewood Cliffs, New Jersey, 1965.

[82] J.G. Jálon, E. Bayo, Kinematic and Dynamic Simulations of Multibody Systems—The Real-Time Challenge, Springer Verlag, New York, 1994.
[83] L. Shampine, M. Gordon, Computer Solution of Ordinary Differential Equations: The Initial Value Problem, Freeman, San Francisco, California, 1975.
[84] K.A. Atkinson, An Introduction to Numerical Analysis, 2nd edition John Wiley & Sons, New York, 1989.
[85] C. Glocker, On frictionless impact models in rigid-body systems, Philosophical Transactions: Mathematical, Physical and Engineering Sciences 359 (2001) 2385–2404.
[86] M. Machado, P. Flores, J.C.P. Claro, J. Ambrósio, M. Silva, A. Completo, H.M. Lankarani, Development of a planar multi-body model of the human knee joint, Nonlinear Dynamics 60 (2010) 459–478.
[87] G. Gilardi, I. Sharf, Literature survey of contact dynamics modeling, Mechanism and Machine Theory 37 (2002) 1213–1239.
[88] G. Hippmann, An algorithm for compliant contact between complexly shaped bodies, Multibody System Dynamics 12 (2004) 345–362.
[89] P. Flores, J. Ambrósio, On the contact detection for contact–impact analysis in multibody systems, Multibody System Dynamics 24 (2010) 255–280.
[90] D.S. Lopes, M.T. Silva, J.A. Ambrósio, P. Flores, A mathematical framework for rigid contact detection between quadric and superquadric surfaces, Multibody System Dynamics 24 (2010) 103–122.
[91] C. Glocker, Concepts for modeling impacts without friction, Acta Mechanica 168 (2004) 1–19.
[92] K.L. Johnson, One hundred years of Hertz contact, Proceedings of the Institution of Mechanical Engineers 196 (1982) 363–378.
[93] ESDU 78035 Tribology Series, Contact Phenomena. I: Stresses, Deflections and Contact Dimensions for Normally Loaded Unlubricated Elastic Components, Engineering Sciences Data Unit, London, England, 1978.
[94] S. Shivaswamy, H.M. Lankarani, Impact analysis of plate using quasi-static approach, Journal of Mechanical Design 119 (1997) 376–381.
[95] R. Cross, The bounce of a ball, American Journal of Physics 67 (1999) 222–227.
[96] T.M. Guess, L.P. Maletsky, Computational modelling of a total knee prosthetic loaded in a dynamic knee simulator, Medial Engineering & Physics 27 (2005) 357–367.
[97] H.M. Lankarani, P.E. Nikravesh, Continuous contact force models for impact analysis in multibody systems, Nonlinear Dynamics 5 (1994) 193–207.
[98] P. Flores, J. Ambrósio, J.C.P. Claro, H.M. Lankarani, Translational joints with clearance in rigid multi-body systems, Journal of Computational and Nonlinear Dynamics 3 (2008) 0110071, 10 pages.
[99] C.M. Pereira, A.L. Ramalho, J.A. Ambrósio, A critical overview of internal and external cylinder contact force models, Nonlinear Dynamics 63 (2011) 681–697.
[100] J. Brändlein, P. Eschamann, L. Hasbargen, Die Wälzlagerpraxis, Handbuch für die Berechnung und Gestaltung von Lagerungen, Vereinigte Fachverlage, Germany, 1998.
[101] G. Nijen, On the overrolling of local imperfections in rolling bearings, Ph.D. Dissertation, University of Twente, The Netherlands, 1997.
[102] H. Minamoto, S. Kawamura, Moderately high speed impact of two identical spheres, International Journal of Impact Engineering 38 (2011) 123–129.
[103] D.C.H. Yang, Z.S. Sun, A rotary model for spur gear dynamics, Journal of Mechanisms, Transmissions and Automation in Design 107 (1985) 529–535.
[104] S. Dubowsky, F. Freudenstein, Dynamic analysis of mechanical systems with clearances, Part 1: formulation of dynamic model, Journal of Engineering for Industry 93 (1971) 305–309.
[105] L.E. Goodman, L.M. Keer, The contact stress problem for an elastic sphere indenting an elastic cavity, International Journal of Solids and Structures 1 (1965) 407–415.
[106] C. Liu, K. Zhang, L. Yang, Normal force–displacement relationship of spherical joints with clearances, Journal of Computational and Nonlinear Dynamics 1 (2006) 160–167.
[107] C. Liu, K. Zhang, L. Yang, The compliance contact model of cylindrical joints with clearances, Acta Mechanica Sinica 21 (2005) 451–458.
[108] Q. Tian, C. Liu, M. Machado, P. Flores, A new model for dry and lubricated cylindrical joints with clearance in spatial flexible multibody systems, Nonlinear Dynamics 64 (2011) 25–47.
[109] C. Liu, K. Zhang, R. Yang, The FEM analysis and approximate model for cylindrical joints with clearances, Mechanism and Machine Theory 42 (2007) 183–197.
[110] L. Luo, M. Nahon, Development and validation of geometry-based compliant contact models, Journal of Computational and Nonlinear Dynamics 6 (2011) 0110041, 11 pages.
[111] Y. Bei, B.J. Fregly, Multibody dynamic simulation of knee contact mechanics, Medical Engineering & Physics 26 (2004) 777–789.
[112] A. Pérez-González, C. Fenollosa-Esteve, J.L. Sancho-Bru, F.T. Sánchez-Marín, M. Vergara, P.J. Rodríguez-Cervantes, A modified elastic foundation contact model for application in 3D models of the prosthetic knee, Medical Engineering & Physics 30 (2008) 387–398.
[113] S. Mukras, A. Mauntler, N.H. Kim, T.L. Schmitz, W.G. Sawyer, Evaluation of contact force and elastic foundation models for wear analysis of multibody systems, Proceedings of the ASME 2010 International Design Engineering Technology Conferences, August 15-18, Montreal, Quebec, Canada, Paper No: DETC2010-28750, 2010.
[114] P. Krempf, J. Sabot, Identification of the damping in a Hertzian contact from experimental non-linear response curve, Proceedings of the IUTAM Symposium on Identification of Mechanical Systems, University of Wuppertal, Germany, 1993.
[115] J. Sabot, P. Krempf, C. Janolin, Nonlinear vibrations of a sphere-plane contact excited by a normal load, Journal of Sound and Vibration 214 (1998) 359–375.
[116] K.L. Johnson, Energy dissipation at spherical surfaces in contact transmitting oscillating forces, Journal of Mechanical Engineering Science 3 (1961) 362–368.
[117] J.E. Shigley, C.R. Mischke, Mechanical Engineering Design, McGraw-Hill, New York, 1989.
[118] S. Dubowsky, F. Freudenstein, Dynamic analysis of mechanical systems with clearances, Part 2: dynamic response, Journal of Engineering for Industry 93 (1971) 310–316.
[119] S. Dubowsky, T.N. Gardner, Design and analysis of multilink flexible mechanism with multiple clearance connections, Journal of Engineering for Industry 99 (1977) 88–96.
[120] T. Kakizaki, J.F. Deck, S. Dubowsky, Modeling the spatial dynamics of robotic manipulators with flexible links and joint clearances, Journal of Mechanical Design 115 (1993) 839–847.
[121] S. Dubowsky, S.C. Young, An experimental and theoretical study of connection forces in high-speed mechanisms, Journal of Engineering for Industry 97 (1975) 1166–1174.
[122] R.J. Rogers, G.C. Andrews, Dynamic simulation of planar mechanical systems with lubricated bearing clearances using vector-network methods, Journal of Engineering for Industry 99 (1977) 131–137.
[123] Y.A. Khulief, A.A. Shabana, A continuous force model for the impact analysis of flexible multibody systems, Mechanism and Machine Theory 22 (1987) 213–224.
[124] S. Hegazy, H. Rahnejat, K. Hussain, Multi-body dynamics in full-vehicle handling analysis under transient manoeuvre, Proceedings of the Institution of Mechanical Engineers, Part K: Journal of Multi-body Dynamics 213 (1999) 19–31.
[125] B. Fox, L.S. Jennings, A.Y. Zomaya, Numerical computation of differential-algebraic equations for non-linear dynamics of multibody systems involving contact forces, Journal of Mechanical Design 123 (2001) 272–281.
[126] S. Dubowsky, J.F. Deck, H. Costello, The dynamic modeling of flexible spatial machine systems with clearance connections, Journal of Mechanisms, Transmissions, and Automation in Design 109 (1987) 87–94.
[127] P.T. Bibalan, R. Featherstone, A study of soft contact models in simulink, Proceedings of the Australasian Conference on Robotics and Automation (ACRA), December 2-4, Sydney, Australia, 2009, 8 pp.
[128] R.W.G. Anderson, A.D. Long, T. Serre, Phenomenological continuous contact–impact modelling for multibody simulations of pedestrian-vehicle contact interactions based on experimental data, Nonlinear Dynamics 58 (2009) 199–208.
[129] Y. Zhang, I. Sharf, Validation of nonlinear viscoelastic contact force models for low speed impact, Journal of Applied Mechanics 76 (2009) 0510021, 12 pages.
[130] P.C. Silva, M.T. Silva, J.M. Martins, Evaluation of the contact forces developed in the lower limb/orthosis interface for comfort design, Multibody System Dynamics 24 (2010) 367–388.

[131] T.M. Guess, G. Thiagarajan, M. Kia, M. Mishra, A subject specific multibody model of the knee with menisci, Medical Engineering & Physics 32 (2010) 505–515.
[132] S. Papetti, F. Avanzini, D. Rocchesso, Numerical methods for a nonlinear impact model: a comparative study with closed-form corrections, IEEE Transactions on Audio, Speech, and Language 19 (2011) 2146–2158.
[133] R.G. Herbert, D.C. McWhannell, Shape and frequency composition of pulses from an impact pair, Journal of Engineering for Industry 99 (1977) 513–518.
[134] N. Sarkar, R.E. Ellis, T.N. Moore, Backlash detection in geared mechanisms: modelling, simulation and experiments, Mechanical Systems and Signal Processing 11 (1997) 391–408.
[135] S. Shivaswamy, Modeling contact forces and energy dissipation during impact in multibody mechanical mystems, Ph.D. Dissertation, Wichita State University, Wichita, Kansas, 1997.
[136] H.S. Lee, Y.S. Yoon, Impact analysis of flexible mechanical system using load-dependent ritz vectors, Finite Elements in Analysis and Design 15 (1994) 201–217.
[137] A.P. Ivanova, Bifurcations in impact systems, Chaos, Solitons & Fractals 10 (1996) 1615–1634.
[138] T.M. Wasfy, A.K. Noor, Computational strategies for flexible multibody systems, Applied Mechanics Reviews 56 (2003) 553–613.
[139] A.L. Schwab, J.P. Meijaard, P. Meijers, A comparison of revolute joint clearance model in the dynamic analysis of rigid and elastic mechanical systems, Mechanism and Machine Theory 37 (2002) 895–913.
[140] P. Flores, J. Ambrósio, J.C.P. Claro, H.M. Lankarani, Dynamic behaviour of planar rigid multibody systems including revolute joints with clearance, Proceedings of the Institution of Mechanical Engineers, Part K: Journal of Multi-body Dynamics 221 (2007) 161–174.
[141] C.M. Pereira, J.A. Ambrósio, A.L. Ramalho, A methodology for the generation of planar models for multibody chain drives, Multibody System Dynamics 24 (2010) 303–324.
[142] M. Boos, J. McPhee, Volumetric contact models and experimental validation, Proceedings of the 1st Joint International Conference on Multibody Dynamics, Lappeenranta, Finland, May 25-27 2010, 10 pp.
[143] M. Boos, J. McPhee, Volumetric contact dynamics models and experimental validation of normal forces for simple geometries, Proceedings of the ASME 2011 International Design Engineering Technology Conferences & Computers and Information in Engineering Conference, August 29-31, Washington, DC, USA, Paper No: DETC2011-49016, 2011.
[144] Q. Zhiying, L. Qishao, Analysis of impact process based on restitution coefficien, Journal of Dynamics and Control 4 (2006) 294–298.
[145] A.S. Yigit, A.G. Ulsoy, R.A. Scott, Spring-dashpot models for the dynamics of a radially rotating beam with impact, Journal of Sound and Vibration 142 (1990) 515–525.
[146] A.S. Yigit, A.P. Christoforou, M.A. Majeed, A nonlinear visco-elastoplastic impact model and the coefficient of restitution, Nonlinear Dynamics 66 (2011) 509–521.
[147] C. Thornton, Coefficient of restitution for collinear collisions of elastic-perfectly plastic spheres, Journal of Applied Mechanics 64 (1997) 383–386.
[148] D. Gugan, Inelastic collision and the Hertz theory of impact, American Journal of Physics 68 (2000) 920–924.
[149] E. Falcon, C. Laroche, S. Fauve, C. Coste, Behaviour of one elastic ball bouncing repeatedly off the ground, The European Physical Journal B 3 (1998) 45–57.
[150] E. Rigaud, J. Perret-Liaudet, Experiments and numerical results on non-linear vibrations of an impacting Hertzian contact. Part 1: harmonic excitation, Journal of Sound and Vibration 265 (2003) 289–307.
[151] G. Kuwabara, K. Kono, Restitution coefficient in a collision between two spheres, Japanese Journal of Applied Physics 26 (1987) 1230–1233.
[152] H. Minamoto, S. Kawamura, Effects of material strain rate sensitivity in low speed impact between two identical spheres, International Journal of Impact Engineering 36 (2009) 680–686.
[153] J. Kagami, K. Yamada, T. Hatazawa, Contact between a sphere and a rough plate, Wear 87 (1983) 93–105.
[154] L. Pust, F. Peterka, Impact oscillator with Hertz's model of contact, Meccanica 38 (2003) 99–116.
[155] L. Vu-Quoc, X. Zhang, L. Lesburg, A normal force–displacement model for contacting spheres accounting for plastic deformation: force-driven formulation, Journal of Applied Mechanics 67 (2000) 363–371.
[156] L. Vu-Quoc, X. Zhang, L. Lesburg, Normal and tangential force–displacement relations for frictional elasto-plastic contact of spheres, International Journal of Solids and Structures 38 (2001) 6455–6490.
[157] L.V. Burgin, R.M. Aspden, Impact testing to determine the mechanical properties of articular cartilage in isolation and on bone, Journal of Materials Science. Materials in Medicine 19 (2008) 703–711.
[158] M.H. Bordbar, T. Hyppänen, Modeling of binary collision between multisize viscoelastic spheres, Journal of Numerical Analysis, Industrial and Applied Mathematics 2 (2007) 115–128.
[159] N. Yoshioka, A review of the micromechanical approach to the physics of contacting surfaces, Tectonophysics 277 (1997) 29–40.
[160] P. Villaggio, The rebound of an elastic sphere against a rigid wall, Journal of Applied Mechanics 63 (1996) 259–263.
[161] R. Ramírez, T. Pöschel, N.V. Brilliantov, T. Schwager, Coefficient of restitution of colliding viscoelastic spheres, Physical Review E 60 (1999) 4465–4472.
[162] C.-Y. Wu, L.-Y. Li, C. Thornton, Energy dissipation during normal impact of elastic and elastic-plastic spheres, International Journal of Impact Engineering 32 (2005) 593–604.
[163] C.-Y. Wu, L.-Y. Li, C. Thornton, Rebound behaviour of spheres for plastic impacts, International Journal of Impact Engineering 28 (2003) 929–946.
[164] X. Shi, A.A. Polycarpou, Measurement and modeling of normal contact stiffness and contact damping at the meso scale, Journal of Vibration and Acoustics 127 (2005) 52–60.
[165] Y. Tatara, N. Moriwaki, Study on impact of equivalent two bodies: coefficients of restitution of spheres of brass, lead, glass, porcelain and agate, and the material properties, Bulletin of Japan Society of Mechanical Engineers 25 (1982) 631–637.
[166] Y. Tatara, Extensive theory of force–approach relations of elastic spheres in compression and in impact, Journal of Engineering Materials and Technology 111 (1989) 163–168.
[167] M. Machado, P. Flores, J. Ambrósio, A. Completo, Influence of the contact model on the dynamic response of the human knee joint, Proceedings of the Institution of Mechanical Engineers, Part K: Journal of Multi-body Dynamics 225 (4) (2011) 344–358.
[168] G. Yamaguchi, Dynamic Modeling of Musculoskeletal Motion, Kluwer Academic Publishers, Dordrecht, The Netherlands, 2001.
[169] M.H. Moeinzadeh, A.E. Engin, N. Akkas, Two-dimensional dynamic modeling of human knee joint, Journal of Biomechanics 316 (1983) 253–264.
[170] G. Li, O. Lopez, H. Rubash, Variability of a three-dimensional finite element model constructed using magnetic resonance images of a knee for joint contact stress analysis, Journal of Biomechanical Engineering 123 (2001) 341–346.